Author's response to review of "Description and validation of an intermediate complexity model for ecosystem photosynthesis and evapo-transpiration: ACM-GPP-ETv1"

Reviewer comments are written in normal black text, authors responses are written in blue while new text in the manuscript in *italics*.

We thank both reviewers for their thorough and encouraging comments on our manuscript. We broadly agree with the comments given and have worked to revise the manuscript to bring clarity to our objectives, explain the novelty of our approach and to highlight the pathways of information transfer between our modelling tools and useful ecological information.

In terms of our motivation, we note that models are often updated with added complexity, whereas we should challenge ourselves to create simpler models. Simpler models are: 1) faster running (fewer calculations); 2) easier to understand (less code); 3) more focused (fewer routines). Simplification means models can be more thoroughly explored, shared, calibrated and tested. Further, we are interested in models with ecological relevant parameters and state variables, such as rooting depth, hydraulic resistance, and LAI. Parameters that are measurable from space, or have values in plant trait databases that can serve as priors, are particularly valuable and were prioritised in our activity here.

Reviewer 1: Martin De Kauwe

Smallman and Williams describe a daily, canopy-scale, coupled photosynthesis-ET model, which they categorise as "intermediate" complexity. They ask how computationally efficient their simpler model is and whether this approach can adequately simulate the complex TEM. They also discuss potential research applications of this model.
The bottom line is that I think this paper is interesting, thorough and I can already see many future applications - it warrants publication. However, I think the current presentation sells it a little short.

For example, the paper starts out by make strong claims for the need for a computational efficient model - fine. But if that is the desire, why not simply use a big-leaf/2-leaf, coupled A-ET model? Or even more simply, a linear approximation (e.g. Best et al. 2015J. Hydrometeor., 16, 1425–1442), or something between those two approaches involving machine learning? My guess, is that the reason is that speed isn't the ultimate objective. So being told that the new model is ~2200 times faster than SPA, to me, isn't all that interesting. I bet I could make a simpler model than this which is quicker still. I'm not arguing that the choices made by Smallman and Williams aren't perfectly legitimate (although "fewer parameters than typical leaf-scale stomatal models" - is that actually true?); however, they aren't simply with speed in mind.

Thank you for your comment Martin. Indeed speed is not the only criterion we aimed to achieve with the development of ACM-GPP-ET. It is clear than we have not sufficiently brought forward our parallel objectives of a more computationally efficient modelling approach, but one that is

still process-orientated and capable of generating realistic emergent properties of the plant photosynthesis and water cycles.
We have modified the manuscript in multiple ways to bring forward both clarity on our objectives and the context for why we chose the approach we have used. The modifications include but not limited to:

Clarifying that there are multiple coupling points between the plant carbon and water cycles at both the stomata scale and also at the root-soil interface:

P2 L8-12: *"Access to CO2 is controlled via leaf stomata, which provide the primary coupling point between GPP and the water cycle. Stomatal opening results in water loss via transpiration creating a dependency on accessible soil moisture, which is controlled by root biomass and its distribution through the soil profile. Thus, the root-soil interface is a second coupling point between the plant carbon and water cycles (Beer et al., 2009; Bonan and Doney, 2018).*"

Clarify that complex models being slow is from the perspective of carrying out large ensemble based analyses:

P2 L24-26: *"However, the increasing complexity of TEMs presents new challenges. Many of the most complex TEMs are too slow for use in model-data fusion analyses which are reliant on massive ensemble simulations (e.g., Ziehn et al., 2012; Smallman et al., 2017)."*

Clarifying that any simplifications must still allow for realistic simulation of the interactions between plant carbon and water cycles to ensure appropriate simulation of emergent responses:

P3 L6-7: "*The challenge here is to produce a model both sufficiently mechanistic to represent the coupling between plant carbon and water cycles linking to ecophysiological processes and observations of key global unknowns (e.g. rooting depth), but also computationally fast enough to be integrated into model-data fusion schemes and to allow a full exploration of parameter-related uncertainties.*"

Further we have variously modified paragraph three of the introduction to highlight some of the challenges surrounding even simpler approaches, such as over sensitivity to drought when using a single layer "bucket" and the breakdown in realism when comparing separate independently calibrated GPP and ET models. Thus, we emphasise the need to have the right estimates of GPP and ET for the *right* reasons.

P3 L8-24: "*Photosynthesis is often estimated using physiologically realistic light, CO2 and temperature response functions (e.g., Jones, 1992; Williams et al., 1997). Evaporation is frequently estimated using simplified versions of the Penman-Monteith model, typically modelling plant stomatal regulation as a function of environmental drivers (e.g., Priestley and Taylor , 1972; Fisher et al., 2008). The impact of moisture limitations on both GPP and ET is* *commonly achieved through the use of VPD as a proxy (e.g., Mu et al., 2011; Wang et al., 2017) or using a single soil layer "bucket" (e.g., Martens et al., 2017). While simple models can show skill when compared to in-situ estimates (Mu et al., 2011; Bloom and Williams , 2015; Martens et al., 2017; Wang et al., 2017) they usually estimate a single process, either photosynthesis or evapo-transpiration, neglecting their coupling. Without coupling, the feedbacks between C and water cycles will not be modelled robustly. For instance, there is a high risk that independently calibrated, simple GPP and ET models that are coupled naively in a plant-soil model framework will misdiagnose the sensitivity of water use efficiency (C fixed per water transpired) and have low predictive capability outside of the calibrated range (e.g., big leaf vs multiple leaf canopy; Tuzet et al., 2003; Wang and Leuning, 1998). Thus, connecting a series of simple models to generate a model of intermediate complexity (IC) carries significant risks. The IC model must represent process interactions effectively. A key test therefore is that any IC model must reproduce the sensitivities of key processes (i.e. GPP, ET,), their interactions (WUE) and soil moisture status demonstrated by the state-of-the-art TEMs, to ensure flux estimates are not only right but right for the right reasons*"

I would like to see more text devoting to the justification of their intermediate model.

Furthermore, we have added a new paragraph specifically detailing the previous works upon which our current study was based. We include reference to gaps in our current modelling tools, linking to globally important unknowns, which ACM-GPP-ET is specifically intended to address:

P3 L25-P4 L8: "*This study builds on two previously developed aggregated canopy models (ACM) for GPP (Williams et al., 1997) and ET (Fisher et al., 2008), and an existing state-of-the-art TEM SPA (Williams et al., 1996; Smallman et al., 2013). ACM-GPP simulated daily GPP sensitive to canopy nitrogen (N), temperature, absorbed shortwave radiation and atmospheric CO2 concentration; based on physiologically realistic relationships but lacking a representation of the impact of soil moisture availability on photosynthesis. Despite this limitation ACM-GPP has been coupled to the DALEC C-cycle model (Williams et al., 2005) and successfully used in model-data fusion experiments to improve our understanding of ecosystem C status, C allocation and residence times (Fox et al., 2009; Bloom and Williams , 2015; Bloom et al., 2016; Smallman et al., 2017) but also carbon-nitrogen interactions (Thomas and Williams et al., 2014). In addition to lacking a soil moisture response on photosynthesis, ACM-GPP limits the capacity of DALEC analyses to constrain the root component of the C cycle as roots currently play no ecological role within the modelling system (i.e. water or nutrient uptake). ACM-ET simulates the bulk ecosystem evapotranspiration based on a modified Penman-Monteith approach sensitive to absorbed shortwave radiation, temperature, vapour pressure deficit and wind speed. However, ACM-ET's bulk approach does not allow for distinguishing between different evaporative sources (i.e. soil surface, root extracted and canopy intercepted rainfall). Thus, it does not account for the different biotic and abiotic drivers which have varied responses to environmental change (Wei et al., 2017). Moreover, ACM-ET does not have a mechanistic coupling to water supply governed by root biomass and root vertical distribution. ACM-GPP and ACM-ET use different empirical models linking LAI,* *minimum tolerated leaf water potential and meteorological drivers to estimate canopy conductance. Both ACM's can be calibrated to provide useful GPP and ET estimates, however when combined their predictive capacity for emergent properties such as WUE is limited (R2 < 0.2; data not shown) highlighting the need for further development to reproduce emergent ecosystem properties."*

And how is the reduction in complexity affecting performance? My sense as a reader is I don't really know the answer to this question after reading the results. In Fig 3, the simpler model produces an R2 > 0.81 for all four fluxes. How much more would this have been degraded by simplifying the model further? Or phrased another way, which of the key assumptions are responsible for this performance? Knowing that might be really insightful for model development and a broader audience than users of the ACM/SPA models. It might also help identify areas where the emulator model could be improved further to be more mechanistic.

Thank you Martin for highlighting the need for clarity over what degree of predictive capacity is expected from the current model and what are the key development components of ACM-GPP-ET. We have addressed this in two components, first a clear statement of the expectations of the ACM-GPP-ET capacity in terms of validation against SPA and against the independent FLUXNET2015 information, and second what the lessons learned from the process.

Question 2 from the end of the introduction has been modified to remind the reader of the importance of key emergent properties not just GPP and ET fluxes.

P4 L30-31: "*How well can the intermediate complexity ACM-GPP-ET emulate the complex TEM (i.e. GPP, ET, their coupling via WUE, and soil moisture)?*"

We have modified the description of the validation process, Section 4, to improve clarity of the different phases of the validation process, their purpose and an explicit hypothesis regarding the performance against FLUXNET2015 sites. For example:

P23 L1-2:*"Therefore, we hypothesise that both SPA and ACM-GPP-ET will perform best at forest sites and less well at sites with different hydraulic traits."*

To highlight key learnings in the model development process Section 6.1 has been reformed to focus on "lessons learnt" rather than computational efficiency:

P28 L4-P29 L15: *"A number of alternate model structures were tested over the course of the development of ACM-GPP-ET, and while it is out of scope to describe these in detail, there are a range of important lessons learned from development of specific components. The single most computationally expensive component is the iterative solution linking photosynthesis and transpiration via stomatal conductance. However, a coupled representation of stomatal conductance linking these processes was essential for maintaining predictive capacity of both* *canopy exchanges and emergent properties of WUE and soil moisture status. Similarly, the simulation of soil moisture dynamics is time-consuming, due to the need for simulating non-linear drainage processes occurring at sub-daily time steps. Water drainage between soil layers and runoff of water from the canopy surface places an upper limit on efficiency achievable while maintaining predictive skill for soil moisture status and indirectly canopy fluxes. However, we expect further efficiency improvements to be achievable through subsequent code modifications including alternate theoretical approaches to achieve the photosynthesis-transpiration coupling. A dedicated focus on code optimality is out of scope for the current study, but is critical to the ongoing process of model improvement.*

In this study 22 parameters are calibrated (Table 3), 15 of these are related to the estimation of canopy and / or soil absorption of PAR, NIR and longwave radiation. The key challenge for the radiative transfer was the essential requirement to reproduce the emergent non-linear functional shape between LAI and canopy radiation absorption, transmittance to soil and reflectance making the complex vertical structure implicit in the calibration. We found that an appropriate simulation of non-linear radiative transfer was critical for realistic radiative responses of each component of evaporation. In contrast, for a GPP model alone a far simpler radiative transfer scheme was viable (Williams et al, 1997). However, the large number of parameters in the radiative transfer scheme is open to constraint through e.g. remote sensing observations of canopy structure and reflectance. These observations could be used to calibrate the scheme for individual locations but also canopy structural forms (i.e. canopy vertical structure).”

Finally, the authors clearly see model-data fusion as a means to calibrate such a model. Therefore, I wonder about some of the choices in terms of mechanism (see point about plant hydraulics).

Our mechanistic focus was strongly prescribed by the structure of the complex TEM, SPA, that was the basis of the process modelling. SPA uses hydraulic functions to set potential and viable rates of liquid water flow, and links these to vapour phase losses. Hydraulic functions are now increasingly studied and linked to vegetation activity and climate sensitivity. Thus there is a developing dataset on hydraulics that the model can connect to.

See responses to specific comments below.

Introduction ————

- Pg 2, line 23: This statement about TEMs being expensive (slow) requires some quantification. It is not my experience that standard TEMs, which simply solve coupled C-water fluxes are actually all that slow. No doubt a model such as SPA (that the second author works with) is undoubtedly slower than most TEMs, but as a blanket statement?

Please see modified text indicated in the response to general comments above to statements on our intended meaning of “slow”

- Pg 2, line 24: the text around issues to do with model data fusion ignores recent advocates of emulators (e.g. Fer, et at. Biogeosciences, 15, 5801-5830, 2018.). (https://www.biogeosciences.net/15/5801/2018/bg-15-5801-2018.pdf)

You are quite right that alternate approaches are available and are entirely viable options. We have modified the manuscript to highlight some of the challenges surrounding alternate calibration approaches to our process emulation strategy:

P2 L26-29: *"While effective and more computationally efficient alternative model-data fusion approaches are available they often reply on model code modifications, such as the creation of the model adjoint in variational approaches (e.g., Kuppel et al., 2012; Raoult et al., 2016), or model emulation often resulting in larger uncertainties in their posterior analysis (e.g., Fer et al., 2018)."*

- Pg 2, line 27-30. Whilst this is a valid argument, I wonder what the evidence is that use of a daily model is less biased than a sub-daily model reliant on a weather generator?

Thank you for the comment we should have provided supporting evidence for this statement. The manuscript has now been modified to contain the following supporting evidence.

P2 L32-P3 L6: *"Finally, there are major challenges in procuring sub-daily meteorological observations needed to drive TEMs away from meteorological stations - this is a particularly acute problem in tropical regions. Thus, TEMs are generally run using statistical down-scaled climate reanalysis data, which contain errors. The uncertainty generated when these errors are propagated into TEM GPP and ET estimates is comparable to IC model error associated with simulating daily fluxes directly(Williams et al., 1997, 2001a). Thus IC models have been shown to have similar errors to TEM models but at a lower computational cost (i.e. 1 time step verses 24 time steps) Thus, there is considerable value in having less complex, fast-running models that simulate GPP and ET."*

This text also ignores a number of papers that have attempted to approximate sub- daily behaviour without the need for a weather generator (e.g. Sands, P. J. (1995). Australian Journal of Plant Physiology 22, 603-6 14.).
Unfortunately we are unable to gain access to the specific example paper. However, we are not aiming to generate sub-daily estimates so the concept of downscaling daily to sub-daily could be considered out-of-scope and potentially confusing to some readers of the current study. Moreover, the abstract for Sands (1995) makes clear that downscaling daily fluxes to sub-daily makes similar assumptions to downscaling meteorology to sub-daily. As discussed in the previous response, such downscaling introduces unavoidable uncertainty.

- Pg 2, Line 31: Agreed and I note that the second author has already produced such a model, ACM. I suggest some text at this point to discuss this and how the proposed approach differs is warranted. Presumably, the distinction is the coupling of the carbon and water cycle and I suggest it is worth including the history of ACM in the discussion on Pg 3.

We agree with this suggestion. Please see the newly added paragraph 4 in the introduction for a detailed introduction of the precursor models.

Methods: ———
- What is the link between eqn 1, Pn and gc, eqn 2? Surely Pn should depend on gc? In fact, the final eqn for GPP, number 14, which is dependent on gc makes sense, but what is the connection to eqn 1 and where is this explained?

Pn refers to the metabolically limited photosynthesis, in the absence of CO2 limitations. This potential sink strength influences the CO2 gradient for exchange between the internal and external environments. This approach follows that used in the original ACM-GPP (Williams et al., 1997) and discussed in Jones (1992). The manuscript is updated in the following ways to make the clear.

Opening to section 2.4:
"*Following Williams et al. (1997) and Jones (1992), GPP is estimated as a co-limited function of temperature, CO2 (limited by stomatal opening and thus plant water availability) and absorbed PAR.* "

To improve clarity in the equations as indicated by both Martin and reviewer #2 the notation have been changed in the following ways (original -> revised)
P_n -> P_{NT}
P_d -> P_{co2}
P -> dayl

Minor corrections to the notation have been made elsewhere in the manuscript and appropriately indicated in the tracked-changes version of the manuscript.

- Where are the equations for gs and gb? I actually see these are included below eqn 57 for gb. It would be worth telling the reader this at the point gs and gb are introduced.

The manuscript has been modified to refer the reader at this point to equation 57 for gb and section 2.6 for gs.

- Page 8, line 5: why is the reference temp 20 and not 25 degrees?

The reference value is as calculated in the source paper (McMurtie et al. (1992)) as stated in the manuscript.
P8L11-12: "*C_{comp} determines the C_i at which GPP becomes positive while C_{half} is the Ci at which CO_2 limited photosynthesis is at 50% of its maximum rate. Both Ccomp and C half are calculated as a function of temperature following McMurtie et al. (1992).*"

- How is the isothermal net radiation estimated?

Isothermal longwave radiation balance calculation is described in sec 2.7.2. The sub-heading as been modified to clarify this. We have also pointed the reader to this in P10 L14.

- Why add in the complexity of the optimisation (sec 2.6) and/or the plant hydraulic resistance (2.9)? Surely this isn't more efficient than a simpler bucket type soil model?

There are several reasons why we chose to use the iWUE optimisation approach to solve our stomatal conductance and to couple this model to multi-layered soil with water supply based on plant hydraulics. First, the iWUE approach, which is also used in SPA, was demonstrated to be more effective under drought conditions than Ball-Berry style approaches (Bonan et al., 2014; see section 2.6). This approach explicitly requires an estimate of water supply. One of the objectives, or rather desired outcomes of the development of ACM-GPP-ET is to connect the roots to photosynthesis to help constrain this component of the carbon cycle, as well as ecosystem traits such as rooting depth (see newly added paragraph 4 of the introduction) but also to link to novel data sources such as SapFlUXNET (P18L3-5). Finally, the choice to use multiple soil layers was driven by the development process. Originally a single layer bucket was tested but was unable to generate reasonable soil moisture dynamics and ultimately drought responses compared with SPA. Incrementally, additional layers were added to improve the soil moisture dynamics. The 4 soil layers is also supported by Blyth and Daamen (1997) who tested different number of soil layers for different soil textures with 4 layers being indicated as the best trade-off on model simplicity and effectiveness.

P28L13-P29L1: "*Originally a single layer bucket was tested but was unable to generate reasonable soil moisture dynamics and ultimately drought responses compared with SPA. Our experience is consistent with other studies which have explicitly considered the impact of varying the number of soil moisture layers (Blyth and Daamen , 1997).*"

Further, in 2.9, the plant hydraulics resistance actually makes little use of commonly measured traits (e.g. p50). I wonder if this isn't quite a disadvantage moving forward. What would any proposed optimisation scheme be calibrating against?

ACM-GPP-ET model structure relies on using hydraulic resistances, which include plant traits which exist within trait databases and are observable (e.g. root resistivity, stem conductance; see Table 3), to estimate the potential hydraulic flow related to the soil water potential and coupling ultimately to atmospheric demand to evaporation. While in this study the parameters listed in Table 3 are not calibrated by the MCMC analysis, they could in the future. Moreover, due to the mechanistic nature the model could estimate equivalents of other frequently measured information such as p50 as emergent properties. Through this avenue such information could be used to improve the calibration.

We believe that this concern has been addressed by the additional introduction provided by paragraph 4 in the introduction but also P18L3-5:

"*The advantage to using a mechanistic approach allows for the estimation of physiological properties which makes possible novel comparisons with field observations such as Poyatos et al. (2016).* "

Results: ——-

- I feel like the start of the results could benefit from a sentence introducing what is happening again. At this point, the manuscript is 22 pages long and although the CARDAMON stuff was introduced in the methods, I suspect you could forgive the reader for being a bit lost. My suggestion would be to re-read 5.1 standalone and see how clear it is for a reader, I would suggest it could be revised.

We now begin the Results section with some summary test:

"*We show that a single global calibration of ACM-GPP-ET can effectively reproduce the patterns of GPP and ET simulated by SPA. Importantly the predictions of WUE are consistent for both ACM and SPA, so that the simplified model is able to capture the interactions between C and water cycling. We also describe an independent validation against FLUXNET data, across 59 sites.*"

- Pg 22: Do the authors have thoughts on why the model is underestimating peaks in transpiration as simulated by SPA?

Implicit to their nature aggregate models are likely to underestimate extremes. In this instance we have the explicit hypothesis that these peaks are missed to due to the lack of energy balance closure of strongly non-linear responses which occur at sub-daily time-scales. We have added text to the discussion to reflect this.

Sec. 6.2: "*ACM-GPP-ET must robustly represent functional forms for C and water cycling across these multiple response dimensions, including any interactions. We note an underestimate in peak transpiration fluxes (Figure 3) which we hypothesise is due to the lack of including the impact of energy balance on canopy and non-linear responses at sub-daily timescales. While this bias may in some cases lead to an underestimate of within day drought / water supply limitation the statistical analyses for validation indicate that the functional forms embedded in ACM-GPP-ET effectively represent those arising from complex mechanistic interactions within SPA. ACM-GPP-ET generates robust daily aggregations from SPA's hourly resolution*"

- Pg 23: "However, ACM-GPP-ET marginally out-performs SPA at most sites and for ET in particular." - how should this be interpreted by the reader? My interpretation is that the simpler model, which is a calibration ought not to out-perform SPA and if it does so, it does so for the wrong reason. This warrants some comment.

We agree that this result does not indicate that ACM-GPP-ET is actually better than SPA, but rather is a result of both random error and potentially as a result of errors in gap-filling the

sub-daily meteorological drivers used in SPA. The manuscript has been modified to include the following in Section 6.3:
"*Indeed, ACM-GPP-ET slightly out-performs SPA in each statistical metric presented here; the greatest difference is found for simulating daily variation of GPP and in particular ET fluxes (Figure 5-6). However, it is unlikely that ACM-GPP-ET has actually improved on SPA itself, as ACM-GPP-ET is an emulation of SPA, therefore the difference should not be viewed as significant. The improved statistics found for ACM-GPP-ET are likely due to a combination of factors underlying errors which by chance lead to an apparent improvement. One exception to this assumption is that SPA's sub-daily meteorological drivers were gap filled based on down-scaled reanalysis drivers (as used in the calibration process) which as noted in the introduction can introduce errors comparable in magnitude to the direct daily aggregation (e.g., Williams et al., 2001a)"*

- I didn't find the comparison in Fig 5 particularly insightful. Lumping all the sites means that we don't learn anything. Where does the model perform best, worst? What does this performance tell us about the underlying mechanisms? In that sense, Figure 7 is more useful and perhaps 5 could be omitted?

We appreciate that this figure is not the most informative, figure 5 along with the density plot component was intended to provide continuity with the results presented in Figure 3 and 4. However, we agree that removing Figure 5 will allow for a smaller paper with a clearer message. The statistics presented alongside of Figure 5 will now be provided in a new Table 4. Figures 6 and 7 have correspondingly been re-numbered

Anonymous Referee #2
The Smallman et al Paper describe a new intermediate complexity model of photosynthesis and evapotranspiration. Such model is partly processes based but using a single canopy layer and daily output is 2000 time faster than full process based models based on half-hourly time steps. The paper is well written. The description of the model, the calibration and validation procedure are sound. The model show good performances compared to the SPA model used for calibration. So I have only few remarks on the model description. However what is missing here is what is really the added value of such a model and what are the final objectives for the development of this model ?

It is stated in the abstract "that model of high complexity cannot be evaluated for their parameter sensitivity nor calibrated thru assimilation of large ensemble" but it is not clear how a model like ACM-GPP-ET can solve this problem? Indeed, they are not based on the same parameters and set of equations so how to infer sensitivity of parameters from the complex model from sensitivity of parameters from intermediate complexity model? Likewise how calibration of intermediate complexity model helps to calibrate complex model (especially in the case on the paper it is the opposite).

Thank you for your comment. It is quite correct that we should be clear in how we can propagate information using ACM-GPP-ET to other models. To inform better inform on this we have added a paragraph to the discussion section.

P32 L23-32: "*The combination of ACM-GPP-ET, coupled to DALEC, and CARDAMOM provide multiple direct and indirect avenues for propagating information acquired using intermediate complexity models to complex state-of-the-art TEMs. ACM-GPP-ET and SPA directly share 5 parameters calibrated in this study (Table 2) plus a further 9 biophysical traits which where not calibrated in this study (Table 3). Moreover, all of the parameters calibrated in this study (Table 2) can be indirectly related to those used in SPA (and many other TEMs) e.g., NUE which is closely related to Vcmax, Jmax and foliar nitrogen, but also radiation absorption/reflectance as a function of LAI. Similarly, when ACM-GPP-ET is combined with DALEC and used within the CARDAMOM framework analyses such as those carried out by Bloom et al. (2016) (as is intended) retrieving information on carbon stocks, carbon allocation and residence times results in retrieval of ecologically relevant traits. These traits can be directly related to parameters found in most state-of-the-art TEMs equipped with a C-cycle. Such information should at a minimum provide information on spatial variation expected, and in the optimum situation inform on the exact magnitude of those parameters.*"

Likewise authors compare results for ACM-GPP-ET to different learning machine algorithms showing similar skill. But then what is the added values of such model compare to machine learning approaches? For me machine learning algorithms, are very well suited to interpolate informations but are difficult to use outside of their domain of training set.

Thank you for your comment. It is important to clarify the advantages of our approach over that of machine learning options. The addition of the new paragraph 4 in the introduction helps to highlight the advantages of a process-oriented approach which would not be possible via a machine learning approach. As you suggest, machine learning approaches are less able to extrapolate, i.e. make prediction outside of their calibration bounds which is essential in climate change related research. To this end Section 6.6 in the discussion has been expanded to include additional objectives of decadal predictions.

See paragraph 4 from introduction above.

P32 L22-32: "*ACM-GPP-ET is well suited for ensemble modelling schemes due to its faster run-time, as shown in the MH-MCMC calibration process used here with SPA outputs used as training data. The parameter posteriors generated here (Figure A1) provide a starting point for full carbon cycle and water cycle analyses across regional to global domains. For instance, Bloom et al. (2016) have shown how an IC GPP model, ACM-GPP (Williams et al., 1997), combined with a carbon cycling model (DALEC; Williams et al., 2005), can be linked into a model-data fusion framework, CARDAMOM. CARDAMOM can, when combined with DALEC, retrieve probabilistic estimates of carbon stocks, fluxes and model parameters (including key unknowns such as photosynthate allocation to plant tissues and their residence times).*

CARDAMOM can produce outputs across a domain at the resolution of input forcing (climate data, burned area) and observational constraints (satellite time series of LAI, biomass maps, soil C maps). The advantage of CARDAMOM is that it generates likelihoods for model initial conditions and parameter values that are consistent with climate forcing and domain observations from e.g. satellites, and their estimated errors. Currently CARDAMOM infers water limitations to C cycling through satellite observations of greenness alone. Because there is no coupling to a local water model, CARDAMOM cannot use modelled information on water balance, or independent observations such as surface soil moisture (e.g., Chen et al., 2018). Through using ACM-GPP-ET in CARDAMOM, it will be possible to assimilate new observational data related to water fluxes and state variables."

On the opposite model, based on process can be extrapolated. Then such model could be used for past or future climate conditions for instance. But ACM-GPP-ET is not a full vegetation model. In particular, it depend of LAI that should be prescribed and not calculated. So simulation are limited to conditions where LAI observations are available. So it would be interesting to know if the final objective is to include such kind of model in a TEM to be able to simulate the complete carbon cycle.

In summary the description of the model and its validation is correct. The model give very satisfying result. But what is really missing in the paper is what are the objective and perspective for such a model.

We are sorry for any confusion, we have not been clear as to the background of our modelling frameworks. We also were not clear about the intended coupling of ACM-GPP-ET to the DALEC C-cycle model, and calibration within the CARDAMOM model-data fusion framework. See various responses above for details.

For more specific points:
- One argument for the intermediate complexity model is the difficulty to have sub-daily climate forcing. I am not very convinced since, first of all most of global products are available at 3 to 6 hourly time steps. Then, even for data only available at daily time- steps, most of the TEM use weather generators to simulate a pseudo diurnal cycle. So this is not really a limit. An interesting question could be to know if intermediate complexity model directly based on daily data are performing better with daily data that more complex models coupled with a weather generator?

We have added a reference which specifically deals with the impact of downscaling meteorology on simulation errors (P2L32-P3L4). With regard to the availability of 3-6 hour information, we argue that there remains advantages to simulation at daily time step as this reduces to computational load substantially when model is used in analyses requiring large ensembles. Please see responses to reviewer 1 for details.

The paper partly reply to this point in the comparison between SPA and ACM-GPP-ET on fluxnet site where ACM-GPP-ET seems to perform a little better that SPA. However the difference is relatively small.

We thank the reviewer for this comment. We do not interpret the results as to mean that ACM-GPP-ET is actually better than SPA, particularly as the differences are small. Rather that errors in the input drivers and the observations underlie these results. See responses to reviewer 1 for the detailed response and modifications to the manuscript.

This first point brings me to a second one about FLUXNET. As ACM-GPP-ET is calibrated on SPA, it will obviously tend to have the same behaviour and then the same discrepancies when compare to FLUXNET (which is visible on Figure 7).So as suggested in the further opportunities it would be interesting to make a calibration of ACM-GPP-ET on observed GPP and ET from fluxnet to see how the calibration differ and how model improve compared to fluxnet.

The discussion text has been expanded to address this possibility in Section 6.6
"*There are an array of next steps to undertake for further development both as a stand alone tool and as part of a coupled modelling framework along with DALEC and CARDAMOM. The ACM-GPP-ET parameters estimated here against SPA can be calibrated individually at FLUXNET2015 site (were sufficient biophysical information are available) to determine critical parameter variability to explain observed differences in fluxes. Driven with remotely sensed LAI ACM-GPP-ET could make global estimates of GPP, ET and WUE for direct comparison with outputs from FLUXCOM, GLEAM and CMIP5 model ensembles. As part of the CARDAMOM framework a site specific FLUXNET2015 analysis allows us to assess our ability to retrieve information on the whole carbon cycle across ecological and climate gradients within a data-rich environment, including key unknowns such as rooting depths which play a critical role in ecosystem resilience to drought. Such analyses provide the supporting frameworks needed to conduct global scale re-analyses and potentially near-term (next 12 months) and intermediate term (next 10 years) predictions with fully resolved uncertainties due to the propagation of ensembles.*"

- I am a little surprised by the calibration protocol making a simulation from 2001 to 2012 with rapid increase of CO2? Since I guess there is some prognostic variables it means that there is correlations between the successive years of simulation and then the rapid (and unrealistic) change in CO2 could lead to artefact in the simulation. So to explore the range of CO2 why not doing a series of simulations from 2001 to 2012 with different (but fixes) levels of CO2?

The calibration is done on individual days (i.e. the model is reset each day, including its prognostic variables) - the goal is to span a range of climate, atmospheric and ecological variability, and that explains the rising CO2 runs we used in SPA. We clarified the text as follows:

“*Atmospheric CO2 concentration for each day was sampled from 300-450 ppm; the exaggerated CO2 range is to ensure that influence of increasing CO2 concentrations is contained within the calibration dataset.*”

- The way LAI is used in the calibration is not clear. It is stated that it is retrieved from DALEC and few lines after it is stated that CARDAMOM assimilate MODIS LAI ? So which LAI is used everyday to force ACM-GPP-ET ? And is the LAI from DALEC is retrieved from a previous simulation or done with a simulation with the same Era-iterim forcing (and CO2 increase) ? this point must be clarified

We apologise for the confusion caused in the description of the calibration and validation. These sections have been revised to clarify the situation. However a brief description is given here. ACM-GPP-ET is calibrated using the CARDAMOM system based on GPP and ET estimates from SPA. Both SPA and ACM-GPP-ET were driven with LAI and root biomass information extracted from a different CARDAMOM analysis which calibrated the DALEC C-cycle model:

“*We used LAI and fine roots datasets Bloom et al. (2016) derived from MODIS LAI products, remotely sensed above ground biomass and ecological process knowledge (for details see; Bloom & Williams 2015.*”

- in equation 12 use P to define day length where different Pn,Pd,Pi represent different GPP limited term is not very appropriate !

The manuscript has been modified accordingly. See response to reviewer 1 for detailed response

Description and validation of an intermediate complexity model for ecosystem photosynthesis and evapo-transpiration: ACM-GPP-ETv1

Thomas Luke Smallman[1,2] and Mathew Williams[1,2]

[1]School of GeoSciences, University of Edinburgh, Edinburgh UK
[2]National Centre for Earth Observations, University of Edinburgh, UK

Correspondence: T.L. Smallman, t.l.smallman@ed.ac.uk

Abstract. Photosynthesis (gross primary production, GPP) and evapo-transpiration (ET) are ecosystem processes with global significance for climate, the global carbon ~~cycle, climate, hydrology~~and hydrological cycles, and a range of ecosystem services. The mechanisms governing these processes are complex but well understood. There is strong coupling between these processes, mediated directly by stomatal conductance and indirectly by root zone soil moisture content and its accessibility. This coupling must be effectively modelled for robust predictions of earth system responses to global change. Yet, it is highly demanding to model leaf and cellular processes, like stomatal conductance or electron transport, with responses times of minutes, over decadal and global domains. Computational demand means models resolving this level of complexity cannot be ~~fully~~easily evaluated for their parameter sensitivity, nor calibrated using earth observation ~~data~~information through data assimilation approaches requiring large ensembles. To ~~resolve this problem~~overcome these challenges, here we describe a coupled photosynthesis evapo-transpiration model of intermediate complexity. The model reduces computational load and parameter numbers by operating at canopy scale and daily time steps. ~~But by including~~Through the inclusion of simplified representation of key process interactions it retains sensitivity to variation in climate, leaf traits, soil states and atmospheric CO_2. The new model is calibrated to match the biophysical responses of a complex terrestrial ecosystem model (TEM) of GPP and ET through a Bayesian model-data fusion ~~process~~framework. The calibrated ACM-GPP-ET generates unbiased estimates of TEM GPP and ET, and captures 80-95 % percent of the sensitivity of carbon and water fluxes by the complex TEM. The ACM-GPP-ET model operates ~~$\sim$2200 times~~three orders faster than the complex TEM. Independent evaluation of ACM-GPP-ET at FLUXNET sites, using a single global parameterisation, shows good agreement with typical R^2 $\sim$0.60 for both GPP and ET. This intermediate complexity modelling approach allows full Monte Carlo based quantification of model parameter and structural uncertainties, global scale sensitivity analyses for these processes, and is fast enough for use within terrestrial ecosystem model-data fusion frameworks requiring large ensembles.

1 Introduction

Ecosystem photosynthesis and evaporation are key ecosystem fluxes, and their strong coupling generates important feedbacks between plant carbon and water cycles (Tuzet et al., 2003; Bonan and Doney, 2018). Ecosystem photosynthesis, or gross primary productivity (GPP) is generally the sole input of organic carbon into terrestrial ecosystems, ultimately determining potential carbon accumulation rates. Ecosystem evaporation, or evapo-transpiration (ET), is the combination of plant mediated transpiration, soil surface evaporation and subsequent evaporation of rainfall intercepted by plant canopies. The dominant abiotic factors governing the magnitude and variability of GPP are temperature, absorbed photosynthetically active radiation (PAR) and CO_2 which are strongly impacted by ~~available~~ leaf area index (LAI). Access to CO_2 is controlled via leaf stomata, which provide the primary coupling point between GPP and the water cycle. Stomatal opening results in water loss via transpiration creating a dependency on ~~available water in the soil, but also~~accessible soil moisture, which is controlled by root biomass and its distribution through the soil profile. Thus, the soil-root interface is a second coupling point between the plant carbon and water cycles (Beer et al., 2009; Bonan and Doney, 2018). State-of-the-art terrestrial ecosystem models (TEMs) provide a mechanistic / process-oriented representation of the coupling between plant carbon and water cycles (e.g. Krinner et al., 2005; Oleson et al., 2010; Smallman et al., 2013; Harper et al., 2016) at leaf or even sub-leaf scale, resolving radiative transfer, stomatal conductance and electron transport. TEMs represent state-of-the-art knowledge on how ecosystems function, and are used to provide meaningful predictions of the responses by and feedbacks from the terrestrial land surface in response to changes in the Earth system (Bonan and Doney, 2018). Mechanistic models linking leaf-level photosynthesis (e.g., Farquhar and von Caemmerer, 1982; Collatz et al., 1991) and transpiration (e.g., Monteith, 1965) through models of stomatal regulation (Medlyn et al., 2011; Williams et al., 1996; Bonan et al., 2014) are well established. Scaling from leaf to canopy scale has grown increasingly complex as the role of non-linear within-canopy variation of both abiotic (e.g., light, temperature, momentum, CO_2 and H_2O) and biotic (i.e. plant traits) factors on plant carbon-water relations has improved (e.g., Wang and Leuning, 1998; Buckley et al., 2013; Sun et al., 2014; Way et al., 2015; Coble et al., 2016; Scartazza et al., 2016; Nolan et al., 2017; Bonan et al., 2018).

However, the increasing complexity of TEMs ~~makes them computationally expensive, which has several drawbacks~~presents new challenges. ~~The slow speed of TEMs hinders their~~Many of the most complex TEMs are too slow for use in model-data fusion analyses which are reliant on massive ensemble simulations (e.g., Ziehn et al., 2012; Smallman et al., 2017). While effective and more computationally efficient alternative model-data fusion approaches are available they often reply on model code modifications, such as the creation of the model adjoint in variational approaches (e.g., Kuppel et al., 2012; Raoult et al., 2016), or model emulation often resulting in larger uncertainties in their posterior analysis (e.g., Fer et al., 2018). ~~Moreover~~ The complexity of typical TEMs generally prevents a robust quantification of their uncertainties; it is very challenging computationally to determine the sensitivities of TEM model outputs to parameter variation. This hinders interpretation of model-data mismatch. Finally, there are major challenges in procuring sub-daily meteorological observations needed to drive~~rs needed for~~ TEMs away from meteorological stations - this is a particularly acute problem in tropical regions. Thus, TEMs are generally run using statistical down-scaled climate reanalysis data~~. Such data necessarily contains~~, which contain ~~a degree of~~ errors ~~which when propagated~~The uncertainty generated when these errors are propagated into TEM GPP and ET estimates is ~~significant compared to other sources of~~comparable to IC model error associated with simulating daily fluxes directly (Williams et al., 1997, 2001a). Thus, IC models have been shown to have similar errors to TEM models but at lower computational cost (i.e. 1 time versus 24 time steps). Thus, there is considerable value in having less complex, fast-running models that simulate GPP and ET. The challenge here is to produce a model *both* sufficiently mechanistic to represent the coupling between plant carbon and water cycles linking to ecophysiological processes and observations of key global unknowns (e.g. rooting depth), but also computationally fast enough to be integrated into model-data fusion schemes and to allow a full exploration of parameter-related uncertainties.

Photosynthesis is often estimated using physiologically realistic light, CO_2 and temperature response functions (e.g., Jones, 1992; Williams et al., 1997)~~, generally using vapour pressure deficit (VPD) as a proxy of moisture stress (e.g., Wang et al., 2017)~~. Evaporation is frequently estimated using simplified versions of the Penman-Monteith model, typically modelling plant stomatal regulation as a function of environmental drivers (e.g., Priestley and Taylor , 1972; Fisher et al., 2008). The impact of moisture limitations on both GPP and ET is commonly achieved through the use of VPD as a proxy (e.g., Mu et al., 2011; Wang et al., 2017) or using a single soil layer "bucket" (e.g., Martens et al., 2017). ~~These simple and highly computationally efficient models can be driven by or combined with satellite based remotely sensed information within data assimilation schemes to constrain carbon or water fluxes at global scales with significant~~While simple models can show skill when compared to in-situ estimates (Mu et al., 2011; Bloom and Williams , 2015; Martens et al., 2017; Wang et al., 2017). ~~However, simple models~~They usually estimate a single process, either photosynthesis or evapo-transpiration, neglecting their coupling. Without coupling, the feedbacks between C and water cycles will not be modelled robustly. For instance, there is a high risk that independently calibrated, simple GPP and ET models that are coupled naively in a plant-soil model framework will ~~not simulate~~misdiagnose the sensitivity of water use efficiency (C fixed per water transpired) and have low predictive capability outside of the calibrated range (e.g., big leaf vs multiple leaf canopy; Tuzet et al., 2003; Wang and Leuning, 1998). Thus, connecting a series of simple models to generate a model of intermediate complexity (IC) carries significant risks. The IC model must represent process interactions effectively. A key test therefore is that any IC model must reproduce the sensitivities of key processes (i.e. GPP, ET), their interactions (WUE) and soil moisture status demonstrated by the state-of-the-art TEMs to ensure flux estimates are right for the *right* reasons.

This study builds on two previously developed aggregated canopy models (ACM) for GPP (Williams et al., 1997) and ET (Fisher et al., 2008), and an existing state-of-the-art TEM SPA (Williams et al., 1996; Smallman et al., 2013). ACM-GPP simulated daily GPP sensitive to canopy nitrogen (N), temperature, absorbed shortwave radiation and atmospheric CO_2 concentration; based on physiologically realistic relationships but lacking a representation of the impact of soil moisture availability on photosynthesis. Despite this limitation ACM-GPP has been coupled to the DALEC C-cycle model (Williams et al., 2005) and successfully used in model-data fusion experiments to improve our understanding of ecosystem C status, C allocation and residence times (Fox et al., 2009; Bloom and Williams , 2015; Bloom et al., 2016; Smallman et al., 2017) but also carbon-nitrogen interactions (Thomas and Williams et al., 2014). In addition to lacking a soil moisture response on photosynthesis ACM-GPP limits the capacity of DALEC analyses to constrain the root component of the C cycle as roots currently play no ecological role within the modelling system (i.e. water or nutrient uptake). ACM-ET simulates the bulk ecosystem evapotranspiration based on a modified Penman-Monteith approach sensitive to absorbed shortwave radiation, temperature, vapour pressure deficit and wind speed. However, ACM-ET's bulk approach does not allow for distinguishing between different evaporative sources (i.e. soil surface, root extracted and canopy intercepted rainfall). Thus, it does not account for the different biotic and abiotic drivers which have varied responses to environmental change (Wei et al., 2017). Moreover, ACM-ET does not have a mechanistic coupling to water supply governed by root biomass and root vertical distribution. ACM-GPP and ACM-ET use different empirical models linking LAI, minimum tolerated leaf water potential and meteorological drivers to estimate canopy conductance. Both ACM's can be calibrated to provide useful GPP and ET estimates, however when combined their predictive capacity for emergent properties such as WUE is limited ($R^2 < 0.2$; data not shown) highlighting the need for further development to reproduce emergent ecosystem properties.

Here we describe a process model of intermediate complexity, ACM-GPP-ET version 1, that simulates gross primary productivity and evapotranspiration. ACM-GPP-ET is a fast, coupled representation of plant carbon and water cycles at ecosystem scale and daily time resolution. Coupling is achieved via a canopy stomatal model that determines CO_2 and H_2O exchanges in the canopy. With fewer parameters than ~~typical leaf-scale stomatal models~~many state-of-the-art process orientated models, our model is simpler to calibrate. With a daily time-step and single canopy layer the model is fast, and therefore viable for ensemble modelling. In fact ACM-GPP-ET is explicitly intended as a replacement for ACM-GPP as part of the DALEC model addressing current weaknesses in simulating carbon-water interactions with our model-data fusion framework. To ensure its realism, ACM-GPP-ET is an emulation of a more complex LSM, SPA (Williams et al., 1996) that resolves leaf scale, hourly exchanges of CO_2 and water. SPA also includes a detailed, multi-layer representation of radiative transfer, energy balance, carboxylation and plant-soil interactions at sub-daily timescales. SPA explicitly couples available supply of water from the soil (determined as a function of soil characteristics, root biomass and structure) to demand by the atmosphere (as a function of absorbed radiation and vapour pressure deficit) which results in robust dynamics in response to varied water availability (Bonan et al., 2014). We create a very large ensemble of SPA runs across environmental space to map the sensitivity of GPP and ET to biophysical changes, and then fit the parameters of ACM-GPP-ET to theses surfaces.

ACM-GPP-ET is based on previous approaches developed to estimate GPP and ET independently (Williams et al., 1997; Fisher et al., 2008), but here uniquely are realistically coupled for the first time. GPP is estimated as a function of foliar nitrogen content allocated to photosynthetic activity, temperature, intercellular CO_2 concentration and absorbed PAR. ET is estimated as the sum of transpiration, evaporation from the soil surface and of rainfall intercepted by the canopy, within a soil water mass balanced system. Using a combination of GPP and ET estimates from both TEM and observation-orientated analyses spanning site to global scales we calibrate and validate ACM-GPP-ET and address the following questions:

1) How computationally efficient is ACM-GPP-ET compared to our complex TEM at estimating daily fluxes?

2) How well can the intermediate complexity ACM-GPP-ET emulate the complex TEM (i.e. GPP, ET, their coupling via WUE and soil moisture)?

3) How do ACM-GPP-ET predictions compare to fully independent FLUXNET derived estimates of carbon and water fluxes across the globe?

Finally we discuss novel research applications made possible using our intermediate complexity, ecophysiologically-based modelling approach including full Monte Carlo based quantification of model parameter and structural uncertainties, global scale sensitivity analyses (e.g. WUE response to increased CO_2), rapid testing of alternate theoretical models of stomatal conductance, and use within terrestrial ecosystem model-data fusion frameworks.

2 Description of ACM-GPP-ET

2.1 Model Overview

The Aggregated Canopy Model for Gross Primary Productivity and Evapo-Transpiration version 1 (ACM-GPP-ET v1) provides a computationally efficient yet broadly mechanistic representation of photosynthetic and evaporative fluxes of terrestrial ecosystems. Evapo-transpiration is explicitly represented as the sum of transpiration (coupled to GPP via a mechanistic representation of stomatal conductance), evaporation from the soil surface and evaporation of precipitation intercepted by the canopy. Absorption and reflectance of short- and long-wave radiation are estimated as non-linear functions of LAI. Aerodynamic conductance for canopy and soil surface exchange are estimated as a function of wind speed and canopy structure (LAI and height). ACM-GPP-ET includes a four-layer model of soil water balance. The top three soil layers are accessible to roots which determines the available supply of water to the plant as a function of fine root biomass and their distribution through the soil profile. Soil evaporation is assumed to be supported by the top soil layer only (Figure 1).

2.2 Model Drivers

ACM-GPP-ET requires both meteorological and biophysical information as inputs (Table 1). Most of the needed drivers are widely available from either field observations or global re-analyses. Meteorological drivers are extracted from the European Centre for Medium Range Weather Forecasting (ECMWF) ERA-Interim re-analysis (Dee et al., 2011), while soil textural information are extracted from global interpolations of field inventories (e.g., HWSD; Hiederer and Köchy, 2011). LAI is widely available from satellite based remote sensing such as the NASA generated MODIS product (https://modis.gsfc.nasa.gov/data/dataprod/mod15.php). In contrast, information on below ground biophysical information, such as root stocks and rooting depth, is more challenging to obtain as they are highly spatially variable and not directly observable from space. Simulation models and model-data fusion based C-cycle analyses may simulate root stocks which can provide useful information (e.g., Bloom et al., 2016) while rooting depth information can also be statistically estimated (e.g., Fan et al., 2017).

2.3 Model Parameters

Parameters within ACM-GPP-ET represent a wide range of time-invariant physical, biogeophysical and biogeochemical properties. In this study we calibrate a total of 22 parameters related to nitrogen-use and light-use efficiency, temperature response of photosynthesis, plant water-use efficiency and radiation absorption and reflectance processes (Table 2); these parameters broadly relate to ecosystem traits. Ecosystem traits can be reasonably expected to vary between ecosystems and thus we should

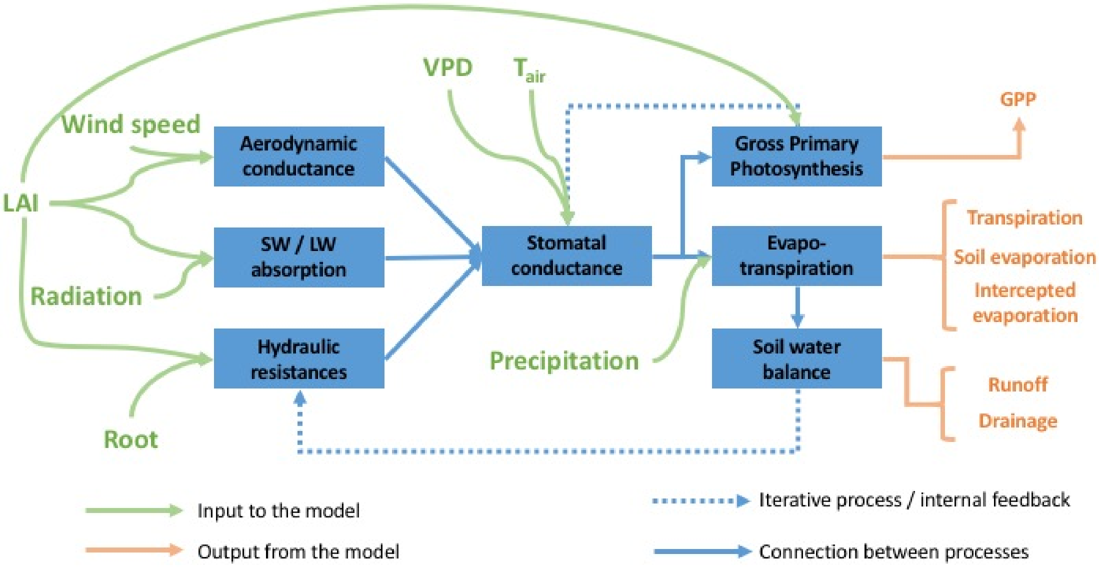

Figure 1. Schematic of ACM-GPP-ET showing its inputs, outputs and how its processes are interconnect. The blue boxes indicate distinct process groupings within the model framework. Green arrows are inputs to the model, while orange arrows indicate model output (i.e. carbon / water fluxes). Blue arrows show the interconnections between the various processes.

be able to retrieve ecologically consistent estimates for these parameters given suitable carbon and water flux information. In this study were we are calibrating against a complex model with 'known' parameter values against which we can compare our estimated values. There are a further 12 biophysical parameters which are assumed to be constant and therefore are not retrieved as part of our calibration procedure (Table 3).

2.4 Gross Primary Productivity

Following Williams et al. (1997) and Jones (1992), GPP is estimated as a co-limited function of temperature, CO_2 (limited by stomatal opening and thus plant water availability) and absorbed PAR. The temperature and foliar nitrogen limited rate of photosynthesis ~~(P_n; gC/m^2/day)~~(P_{NT}; gC/m^2/day) is first determined as a function of leaf area index (LAI; m^2/m^2), average foliage nitrogen content (N_{fol}; gN/m^{2}leaf), nitrogen use efficiency (NUE; gC/gN/m^{2}leaf/day) and temperature (T_{air}; °C).

$$\mathrm{P}_{NT} = \mathrm{LAI} \cdot \mathrm{N}_{fol} \cdot \mathrm{NUE} \cdot T_{adj} \tag{1}$$

Where T_{adj} describes a skewed normal distribution (scaling 0-1) with an optimum (T_{opt}), maximum temperature (T_{max}) and kurtosis ($Kurt$).

$$\mathrm{T}_{adj} = exp\left(log\left(\frac{\mathrm{T}_{max} - \mathrm{T}_{air}}{\mathrm{T}_{max} - \mathrm{T}_{opt}}\right) \cdot Kurt \cdot (\mathrm{T}_{max} - \mathrm{T}_{opt})\right) \cdot exp(Kurt \cdot (\mathrm{T}_{max} - \mathrm{T}_{opt})) \tag{2}$$

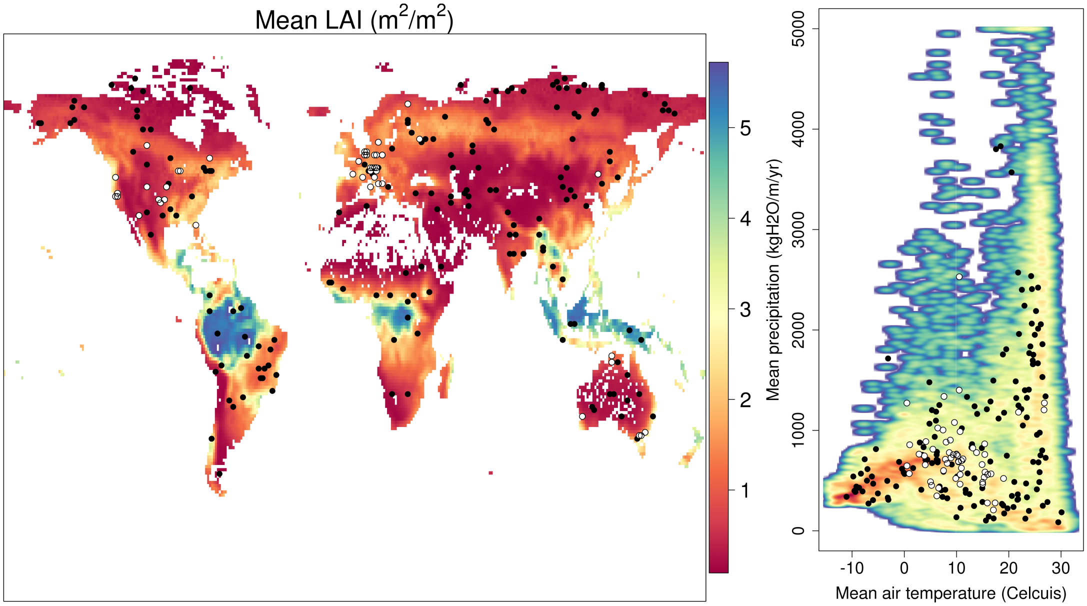

Figure 2. Left global (1 x 1 degree) mean LAI estimates (2001-2015) derived from NASA's MODIS product. Right climate space described by mean annual precipitation and temperature (ECMWF's ERA-Interim; Dee et al., 2011). Shading indicates the point density with red areas indicating high density. In both plots black circles show the location of SPA calibration sites, while the white circles with black ring show the FLUXNET2015 sites used to provide independent validation.

CO_2 limitation is depended on canopy conductance of CO_2 (g_c; $mmolCO_2/m^2/day$) which is assumed to be the combined conductance of the stomata (g_s; $mmolH_2O/m^2/s$) and leaf boundary layer (g_{b-mmol}; $mmolH_2O/m^2/s$). Note, that g_s and g_b are calculated for conductance of water vapour and thus coefficients 1.65 and 1.37 convert conductance of water to those of CO_2 (Jones, 1992), $dayl_{sec}$ = 86400 is the number of seconds per day.

$$g_c = dayl_{sec} \cdot \left(\frac{1}{g_{s-mmol} \cdot 1.65} + \frac{1}{g_{b-mmol} \cdot 1.37} \right)^{-1} \tag{3}$$

The canopy boundary layer (g_b; see Eq. 57) and stomatal conductance (g_s) are initially calculated in m/s, and thus must be converted into $mmolH_2O/m^2/s$ for the purposes of calculating CO_2 exchange. Note that the coupling between photosynthesis and transpiration occurs via g_s which is estimated as a function of available water supply, atmospheric demand and the intrinsic water use efficiency threshold on GPP, see Sec. 2.6 for details on the estimation of g_s.

$$g_{b-mmol} = g_b \cdot (1000 \cdot Pr_{air} / (T_{airK} \cdot R_{con})) \tag{4}$$

$$g_{s-mmol} = g_s \cdot (1000 \cdot Pr_{air} / (T_{airK} \cdot R_{con})) \tag{5}$$

Table 1. Drivers required as inputs by ACM-GPP-ET. Each driver has its unit specified and brief description. The mean value across the calibration climate space is given with the standard deviation in parenthesis. The drivers are divided between those which are time varying and those assumed constant for a given location but can vary between locations.

	Name	Units	Mean (SD)	Description
Time varying				
	Doy	Julian Day	-	Time step median Julian day of year
	Maximum temperature	$^{\circ}$C	14.9 (16.9)	Time step maximum air temperature
	Minimum temperature	$^{\circ}$C	7.3 (15.9)	Time step minimum air temperature
	Short-wave Radiation	MJ/m^2/day	15.0 (8.4)	Time step average daily sum incoming short-wave radiation
	CO_2	ppm or μmol/mol	372.5 (42.7)	Time step mean atmospheric CO_2 concentration
	VPD	Pa	753 (888)	Time step mean water vapour pressure deficit
	Precipitation	kgH_2O/m^2/s	2.7x10^{-6} (9.6x10^{-6})	Time step mean liquid precipitation rate
	Wind Speed	m/s	2.9 (1.8)	Time step mean wind speed
	LAI	m^2/m^2	1.9 (1.3)	Time step specific leaf area index
	Fine root stocks	gC/m^2	151 (105)	Time step specific fine root stocks
Constant				
	D_{root_max}	m	2	Maximum rooting depth
	K_{root}	gbiomass/m^2	150	Root biomass needed to reach 50 % of D_{root_max}
	Soil sand percentage	volumetric percentage	45.8 (16)	Soil sand percentage representative of two depths, 0-30 cm and 31-100 cm
	Soil clay percentage	volumetric percentage	21.4 (8.8)	Soil clay percentage representative of two depths, 0-30 cm and 31-100 cm

Where T_{airK} is the air temperature in Kelvin, Pr_{air} is air pressure (default = 101325 Pa) and R_{con} is the universal gas constant (8.3144 J/K/mol). The scalar 1000 adjusts units from mol to mmol.

The internal CO_2 concentration (C_i; ppm or μmol/mol) is estimated as a function of atmospheric CO_2 concentration (C_a; ppm or μmol/mol), g_c, the CO_2 compensation (C_{comp}; ppm or μmol/mol) and half saturation (C_{half}; ppm or μmol/mol) points.

$$\mathrm{C}_i = \frac{m + (m^2 - 4 \cdot (\mathrm{C}_a \cdot q - p \cdot \mathrm{C}_{comp}))^{0.5}}{2} \tag{6}$$

$$q = \mathrm{C}_{comp} - \mathrm{C}_{half} \tag{7}$$

$$p = (\mathrm{P}_{NT} \cdot \mathrm{M}_{\mathrm{C}}^{-1} \cdot 1\mathrm{x}10^6)/\mathrm{g}_c \tag{8}$$

$$m = \mathrm{C}_a + q - p \tag{9}$$

M_{C} (12 gC/mol) is the molar ratio of carbon, where its inverse ($\mathrm{M}_{\mathrm{C}}^{-1}$ converts from molC to gC and 1x10^6 scales from μmol to mol.

C_{comp} determines the C_i at which GPP becomes positive while C_{half} is the C_i at which CO_2 limited photosynthesis is at 50 % of its maximum rate. Both C_{comp} and C_{half} are calculated as a function of temperature following McMurtie et al. (1992).

$$\mathrm{C}_{comp} = \alpha_{comp} \cdot e^{\beta_{comp} \cdot \frac{\mathrm{T}_{airK} - 298.15}{\mathrm{T}_{airK}}} \tag{10}$$

$$\mathrm{C}_{half} = \alpha_{half} \cdot e^{\beta_{half} \cdot \frac{\mathrm{T}_{airK} - 298.15}{\mathrm{T}_{airK}}} \tag{11}$$

where α_{comp} and α_{half} describe the values at the reference temperature (20^{o}C or 298.15 K) and β_{comp} and β_{half} describe the sensitivity of the temperature response.

Table 2. ACM-GPP-ET parameters retrieved using the CARDAMOM model-data fusion system. For each parameter its symbol as used in the code description is given, along with the maximum and minimum values used for the prior ranges, the maximum likelihood estimate retrieved from the posterior distributions, units and a brief description. The SPA column contains the SPA parameter value used in the calibration where a direct equivalent is available. Near infrared radiation is abbreviated as NIR, photosynthetically active radiation is abbreviated as PAR and long-wave radiation as LW.

Symbol	Prior (min/max)	Posterior	SPA	Units	Description
NUE	3/40	14.9	-	gC/gN/m^{2}leaf/day	Photosynthetic nitrogen use efficiency at optimum temperature, light and CO$_2$ conditions
T$_{max}$	45/60	52.6	56	$^\circ$C	Maximum temperature for photosynthesis
T$_{opt}$	20/40	34.5	30	$^\circ$C	Optimum temperature for photosynthesis
$Kurt$	0.1/0.3	0.13	0.183	-	Kurtosis of temperature response
E$_0$	1/7	4.5		gC/MJ/m^2/day	Quantum yield, C update per unit of photosynthetically active radiation
$min\Psi$	2.5/1.5	2.0	2.0	MPa	Absolute value for minimum tolerated leaf water potential
iWUE	1x10^{-10}/1x10^{-3}	1.6x10^{-6}	8.8x10^{-7}	gC/m^{2}leaf/day/mmolH$_2$O	Intrinsic water use efficiency
$\alpha_{LW-refl}$	0.9/1.0	0.07		-	Maximum fraction of incoming LW radiation reflectance by the canopy
$K_{LW-refl}$	0.01/2.5	0.79		m^2/m^2	LAI at which LW radiation reflectance at 50 % of maximum
$\alpha_{NIR-refl}$	0.1/1.0	0.11		-	Maximum fraction of incoming NIR reflectance by canopy
$K_{NIR-refl}$	0.01/2.5	0.19		m^2/m^2	LAI at which near NIR reflectance by canopy at 50 % of maximum
$\alpha_{PAR-refl}$	0.1/1.0	0.10		-	Maximum fraction of incoming PAR reflectance by canopy
$K_{PAR-refl}$	0.01/2.5	0.23		m^2/m^2	LAI at which PAR reflectance by canopy at 50 % of maximum
$\alpha_{LW-trans}$	0.5/1.0	0.60		-	Maximum fractional reduction of incoming LW radiation transmitted by the canopy
$K_{LW-trans}$	0.01/2.5	0.51		m^2/m^2	LAI at which reduction of LW radiation transmittance is at 50 % of maximum
$\alpha_{NIR-trans}$	0.5/1.0	0.99		-	Maximum fractional reduction of incoming NIR transmitted by canopy
$K_{NIR-trans}$	0.01/2.5	1.85		m^2/m^2	LAI at which reduction of near NIR transmittance is at 50 % of maximum
$\alpha_{PAR-trans}$	0.5/1.0	0.99		-	Maximum fractional reduction of incoming PAR transmitted by canopy
$K_{PAR-trans}$	0.01/2.5	1.76		m^2/m^2	LAI at which reduction of PAR transmittance is at 50 % of maximum
$\alpha_{LW-release}$	0.01/1.0	0.98		-	Maximum fraction of LW radiation emitted by leaf area to be released from the canopy
$K_{LW-release}$	0.01/2.5	0.68		m^2/m^2	LAI at which LW release from the canopy is at 50 % of maximum
$soil_{abs}$	0.5/0.99	0.62	0.98	-	Fraction of incident NIR + PAR absorbed by soil

CO$_2$ limited photosynthesis (P$_{\mathrm{CO2}}$; gC m^{-2} day^{-1}) is calculated as a function of g$_c$ and CO$_2$ exchange gradient. Where 1x10^{-6} scales from μmol to mol while M$_\mathrm{C}$ molar units to gC. At this juncture, a day length (dayl: hours) correction is applied to be consistent with the light limitation calculation which follows

$$\mathrm{P_{CO2}} = (\mathrm{g}_c \cdot (\mathrm{C}_a - \mathrm{C}_i)) \cdot 1\mathrm{x}10^{-6} \cdot \mathrm{M_C} \cdot \frac{\mathrm{dayl}}{24} \tag{12}$$

Light limited photosynthesis (P$_I$; gC/m^2/day) is defined as a function of absorbed short-wave radiation (I) and a quantum yield parameter (E$_0$).

$$\mathrm{P}_I = \mathrm{E}_0 \cdot \mathrm{I} \tag{13}$$

Table 3. Parameters describing physical or biophysical constants not retrieved as part of the CARDAMOM model-data fusion analysis.

Symbol	Value	Units	Description
$PAR:SW$	0.5	-	Fraction of short-wave radiation assumed to be photosynthetically active
σ	0.96	-	Long-wave radiation emissivity of a surface
κ	5.67 x 10^{-8}	W/m^2/K^{-4}	Stefan-Boltzmann constant
d_o	0.08	m	Mean leaf diameter
$Root_{density}$	0.31x10^6	gbiomass/m^3	Mean root density within soil per unit volume (Bonan et al., 2014)
$Root_{radius}$	0.00029	m	Mean root radius (Bonan et al., 2014)
$Root_{Resist}$	25	MPa/s/g/mmolH$_2$O	Mean root resistivity to hydraulic flow (Bonan et al., 2014)
G_p	5	mmol/m^{2}leaf/s/MPa	Mean plant conductivity to hydraulic flow (Bonan et al., 2014)
α_{comp}	36.5	μmol/mol CO$_2$	CO$_2$ compensation point for photosynthesis at 20^{o}C (McMurtie et al., 1992)
α_{half}	310	μmol/mol CO$_2$	CO$_2$ half saturation point for photosynthesis at 20^{o}C (McMurtie et al., 1992)
β_{comp}	282.61	K	Temperature sensitivity parameter for CO$_2$ compensation point (McMurtie et al., 1992)
β_{half}	297.106	K	Temperature sensitivity parameter for CO$_2$ half saturation point (McMurtie et al., 1992)

The final GPP estimate (gC/m^2/day) is the result of combined light and CO$_2$ limited photosynthesis.

$$\text{GPP} = \frac{\text{P}_I \cdot \text{P}_{\text{CO2}}}{\text{P}_I + \text{P}_{\text{CO2}}} \tag{14}$$

2.5 Evapo-transpiration

Evapo-transpiration is based on the Penman-Monteith model assuming isothermal net radiation conditions (Jones, 1992). Evaporation is simulated from three source which are (i) transpiration, (ii) evaporation of precipitation intercepted by the canopy and (iii) the soil surface. The following sections detail the calculation of each evaporative source within their respective available water supplies.

2.5.1 Transpiration

Transpiration (E$_{trans}$; kgH$_2$O/m^2/day) is estimated by the Penman-Monteith equation linking the drivers of transpiration, canopy radiation status and atmospheric demand, with restrictions on evaporative losses, namely available water supply from the roots within the soil profile. The upper limit on water supply is imposed by restricting the maximum stomatal conductance (g$_s$) for a given set of environmental conditions (process described in Sect. 2.6).

$$\text{E}_{trans} = \frac{(s \cdot \Phi_{iso-canopy}) + (\rho_{air} \cdot cp_{air} \cdot \text{VPD} \cdot \text{g}_b)}{\lambda \cdot (s + (\gamma \cdot (1 + \text{g}_b/\text{g}_s)))} \cdot \text{dayl} \cdot 3600 \tag{15}$$

$\Phi_{iso-canopy}$ is the isothermal net radiation (W/m^2; see Section 2.7.2) while s (kPa K^{-1}) is the slope of curve relating saturation vapour pressure with air temperature and γ is the psychrometer constant (kPa K^{-1}). ρ_{air} is the density of air (kg/m^3), λ is the latent heat of vaporisation (J kg^{-1}) and cp_{air} is the specific heat capacity of air (J/kg/K).

s, γ and λ are calculated as a function of T_{air} following equations described in Jones (1992).

$$s = \frac{s_{ref0} \cdot 17.269 \cdot 237.3 \cdot e^{17.269 \cdot \mathrm{T}_{air}/(\mathrm{T}_{air}+237.3)}}{(\mathrm{T}_{air}+237.3)^2} \tag{16}$$

$$\gamma = \gamma_{ref0} \cdot e^{0.00097 \cdot \mathrm{T}_{air}} \tag{17}$$

$$\lambda = \lambda_{ref0} - 2364 \cdot \mathrm{T}_{air} \tag{18}$$

s_{ref0} (0.61078 MPa), γ_{ref0} (0.0646 kPa) and λ_{ref0} (2501000 J/kg) are s, γ and λ at 0^{o}C reference temperature. ρ_{air} is calculated as a function of T_{airK}.

$$\rho_{air} = \frac{353}{\mathrm{T}_{airK}} \tag{19}$$

The calculation of canopy conductance (g_b; m/s) is described in section 2.8.1 linked to canopy properties (LAI and canopy height) and wind speed. Stomatal conductance (g_s; m/s), used in both the calculation of GPP and transpiration, is calculate via an iterative bisection procedure described in the following section.

2.5.2 Wet canopy evaporation

Wet canopy surface evaporation (E_{wet}; kgH$_2$0/m^2/day) is the evaporation of precipitation intercepted by the canopy and thus is limited by the available canopy water storage (C_{stor}).

$$\mathrm{E}_{wet} = \begin{cases} \mathrm{C}_{stor}, & \mathrm{E}_{pot} > \mathrm{C}_{stor} \\ \mathrm{E}_{pot}, & \text{otherwise} \end{cases} \tag{20}$$

Where E_{pot} is the potential wet canopy evaporation (kgH$_2$0/m^2/day). E_{pot} is assumed to be unrestricted evaporation as estimated by the Penman model assuming isothermal net radiation. E_{pot} is further restricted based on the ratio of current canopy water storage

$$\mathrm{E}_{pot} = \left(\frac{(s \cdot \Phi_{iso-canopy}) + (\rho_{air} \cdot cp_{air} \cdot \mathrm{VPD} \cdot \mathrm{g}_b)}{\lambda \cdot (s+\gamma)} \cdot dayl_{sec} \cdot \frac{\mathrm{C}_{stor}}{\mathrm{C}_{max}} \right) \tag{21}$$

Where C_{max} is the maximum canopy water storage (kgH$_2$0/m^2), defined as a function of LAI related by α (0.2) as previously used in SPA (Smallman et al., 2013).

$$\mathrm{C}_{max} = \alpha \cdot \mathrm{LAI} \tag{22}$$

C_{stor} is determine by water inputs from precipitation, less that which reaches the soil surface (i.e. through-fall), and its water losses by evaporation (as described above) or overflow from intercepted water exceeding C_{max} onto the ground. The fraction of precipitation expected to be through-fall (Tfall) is estimated as a function of LAI related by μ (0.5). Where μ is selected assuming that interception if rainfall is similar to that of direct radiation.

$$\mathrm{Tfall} = e^{-\mu \cdot \mathrm{LAI}} \tag{23}$$

2.5.3 Soil surface evaporation

Soil evaporation (E_{soil}; kg$\mathrm{H}_2$0/m^2/day) is estimated using the Penman-Monteith equation linking drivers of evaporation, soil isothermal radiation ($\Phi_{iso-soil}$; W/m^2) and atmospheric demand, with restrictions on evaporative losses (i.e. namely available water in the top soil layer). The upper limits evaporation is also restricted by the thickness of the dry layer (drythick; m) of soil at the surface.

$$\mathrm{E}_{soil} = \frac{(s \cdot \Phi_{iso-soil}) + (\rho_{air} \cdot cp_{air} \cdot \mathrm{VPD}_{soil} \cdot \mathrm{g}_{soil})}{\lambda \cdot (s + (\gamma \cdot (1 + \mathrm{g}_{soil}/\mathrm{g}_{ws})))} \cdot \mathrm{dayl} \cdot 3600 \tag{24}$$

Where g_{soil} is the soil surface aerodynamic conductance (m/s) and g_{ws} is the conductance of water vapour (m/s) through the soil air space. VPD_{soil} is the vapour pressure deficit (kPa) between the air above the soil and air within the soil pore space.

$$\mathrm{g}_{ws} = \frac{\mathrm{por}_{top} \cdot D_w \cdot \left(\frac{\mathrm{T}_{airK}}{293.2}\right)^{1.75}}{\tau \cdot \mathrm{drythick}} \tag{25}$$

Where por_{top} is the porosity (0-1; m^3/m^3) for the top soil layer as calculated using the Saxton model of soil hydrology (Saxton et al., 1986; Williams et al., 2001b), D_w is the diffusion coefficient for water through air (m^2/s) at reference temperature 293.2 K and 1.75 is a scalar coefficient relating the temperature dependence of D_w. τ is the tortuosity (=2.5).

$$\mathrm{VPD}_{soil} = \mathrm{VPD} - e_{surf} \tag{26}$$

$$e_{surf} = e_{sat} - e_{soil} \tag{27}$$

$$e_{soil} = e_{sat} \cdot e^{\frac{1\mathrm{x}10^6 \cdot \mathrm{SWP}_{top} \cdot V_w}{R_{con} \cdot \mathrm{T}_{airK}}} \tag{28}$$

$$e_{sat} = 0.1 \cdot e^{\frac{1.8095 + (17.269 \cdot \mathrm{T}_{airK} - 4717.306)}{\mathrm{T}_{airK} - 35.86}} \tag{29}$$

e_{surf} is the vapour pressure deficit within the soil air space (kPa). e_{soil} is the vapour pressure in the soil air space (kPa) and e_{sat} is the saturation vapour pressure at the current temperature. SWP_{top} is the soil water potential (MPa) for the top soil layer while V_w is the partial molar volume of water at 20 °C (= 1.805x10^{-7} m^3/mol). All other scalar values are coefficients relating current air temperature to e_{sat}.

2.6 Calculating g_s: the coupling point between plant C and $\mathrm{H_2O}$ cycles

The iWUE optimisation approach for estimating g_s is well established and validated, in particular iWUE has been show to show improved drought response of g_s compared to Ball-Berry g_s model Williams et al. (1996); Bonan et al. (2014). The model aims to maximise photosynthetic uptake within the constraints on g_s imposed by the available supply of water to the canopy and atmospheric demand for evaporation, this approach is referred to as optimising the intrinsic water use efficiency (iWUE).

Calculation of g_s is a three step process. Step 1 estimation of the potential steady flow water supply over the day (MaxSupply; $\mathrm{kgH_20/m^2/day}$) from the soil via roots to the canopy.

$$\text{MaxSupply} = \frac{LWP_{min} - \text{wSWP}}{\mathrm{R}_{tot}} \cdot \mathrm{M_{H2O}} \cdot 1\mathrm{x}10^{-3} \cdot dayl_{sec} \tag{30}$$

Where LWP_{min} is the minimum tolerated leaf water potential (MPa), wSWP is the soil water potential weighted by root access (MPa) and R_{tot} is the total hydraulic resistance ($\mathrm{MPa/s/m^2/mmol}$). The unit is changed from mmol to gC using the molar mass of water $\mathrm{M_{H2O}}$ (18 g/mol) and $1\mathrm{x}10^{-3}$ scalar. Step 2 inverts the Penman-Monteith equation to calculate the value of g_s required to meet MaxSupply under current atmospheric demand and isothermal net radiation conditions.

$$\mathrm{g}_{s-max} = \mathrm{g}_b / \frac{\left(\frac{(s\cdot\Phi_{iso-canopy})+(\rho_{air}\cdot cp_{air}\cdot\text{VPD}\cdot\mathrm{g}_b)}{(\lambda\cdot(\text{MaxSupply}/(dayl_{sec}\cdot\frac{dayl}{24})))-s}\right)}{\gamma} \tag{31}$$

Step 3 uses an iterative bisection process which quantifies the sensitivity of GPP to g_s increment by 1 $\mathrm{mmolH_20/m^2/s}$ (δGPP; $\mathrm{gC/m^2leaf/day/mmolH_20g}_s$); between g_s = 0 and g_{s-max} minimising gs_{opt}, the difference between $\delta\mathrm{GPP/g}_s$ and $iWUE$; $\mathrm{gC/m^2leaf/day/mmolH_20g}_s$.

$$\mathrm{gs}_{opt} = \text{iWUE} - \frac{\delta\text{GPP}}{\text{LAI}} \tag{32}$$

2.7 Radiation balance

State-of-the-art radiative transfer schemes are able to quantify differential canopy absorption, transmittance to soil soil surface and reflection back to the sky of PAR, NIR and long-wave radiation. Using a detailed radiative transfer scheme as a base (Williams et al., 1998), here we have developed simple Michaelis-Menten relationships parameterised to reproduce the emergent absorption, transmittance and reflection properties of a canopy as a function of LAI.

Net canopy ($\Phi_{iso-canopy}$; $\mathrm{W/m^2}$) and soil ($\Phi_{iso-soil}$; $\mathrm{W/m^2}$) isothermal radiation balances are calculated from the combination of short- and long-wave absorption detailed in the following sections.

$$\Phi_{iso-canopy} = APAR_{canopy} + ANIR_{canopy} + ALW_{canopy} \tag{33}$$

$$\Phi_{iso-soil} = APAR_{soil} + ANIR_{soil} + ALW_{soil} \tag{34}$$

2.7.1 Short-wave radiation absorption

ACM-GPP-ET uses a bi-directional radiative transfer scheme to estimate the absorption of PAR and NIR by the canopy and soil surface. Downward radiation first interacts with the canopy either being reflected back toward the sky, transmitted toward the soil surface or absorbed by the canopy. Second the radiation which is transmitted through the canopy to the soil surface is either absorbed or reflected back through the canopy.

The fraction of incoming PAR ($canopy_{PAR-abs}$) and NIR ($canopy_{NIR-abs}$) absorbed is estimated as the residual of that reflected back into the sky ($canopy_{PAR-refl}$, $canopy_{NIR-refl}$) or that transmitted ($canopy_{PAR-trans}$, $canopy_{NIR-trans}$)

toward the soil surface.

$$canopy_{PAR-refl} = \frac{\alpha_{PAR-refl} \cdot \text{LAI}}{\text{LAI} + K_{PAR-refl}} \tag{35}$$

$$canopy_{NIR-refl} = \frac{\alpha_{NIR-refl} \cdot \text{LAI}}{\text{LAI} + K_{NIR-refl}} \tag{36}$$

$$canopy_{PAR-trans} = 1 - \frac{\alpha_{PAR-trans} \cdot \text{LAI}}{\text{LAI} + K_{PAR-trans}} \tag{37}$$

$$canopy_{NIR-trans} = 1 - \frac{\alpha_{NIR-trans} \cdot \text{LAI}}{\text{LAI} + K_{NIR-trans}} \tag{38}$$

$$canopy_{PAR-abs} = 1 - canopy_{PAR-refl} - canopy_{PAR-trans} \tag{39}$$

$$canopy_{NIR-abs} = 1 - canopy_{NIR-refl} - canopy_{NIR-trans} \tag{40}$$

where $\alpha_{NIR-refl}$ and $\alpha_{PAR-refl}$ are the maximum fraction of NIR and PAR reflected by the canopy. $K_{NIR-refl}$ and $K_{PAR-refl}$ are the LAI values at which 50 % of maximum reflectance is achieved for NIR and PAR respectively. $\alpha_{NIR-trans}$ and $\alpha_{PAR-trans}$ are the maximum reduction in transmittance for NIR and PAR, similarly $K_{NIR-trans}$ and $K_{PAR-trans}$ are the LAI at which transmittance is reduced by 50 %. Absorption of PAR ($APAR_{canopy}$) and NIR ($ANIR_{canopy}$) by the canopy on its first pass down through the canopy is estimate as

$$APAR_{canopy} = \text{PAR} \cdot canopy_{PAR-abs} \tag{41}$$

$$ANIR_{canopy} = \text{NIR} \cdot canopy_{NIR-abs} \tag{42}$$

Transmitted PAR and NIR is then incident on the soil surface to be absorbed by the soil surface or reflected back up towards the canopy. We assume that the soil absorption fraction ($soil_{abs}$) of incident PAR and NIR are the same, however PAR and NIR remain independently tracked to allow for subsequent reflection back towards the canopy.

$$APAR_{soil} = \text{PAR} \cdot canopy_{PAR-trans} \cdot soil_{abs} \tag{43}$$

$$ANIR_{soil} = \text{NIR} \cdot canopy_{NIR-trans} \cdot soil_{abs} \tag{44}$$

PAR and NIR which is reflected from the soil is then available for a second opportunity of the canopy to absorb, and typically contributed < 1 % of absorbed radiation in ACM-GPP-ET. Therefore the total $APAR_{canopy}$ and $ANIR_{canopy}$ are calculated as follows

$$APAR_{canopy} = APAR_{canopy} + (\text{PAR} \cdot canopy_{PAR-trans} \cdot (1 - soil_{abs}) \cdot canopy_{PAR-abs}) \tag{45}$$

$$ANIR_{canopy} = ANIR_{canopy} + (\text{NIR} \cdot canopy_{NIR-trans} \cdot (1 - soil_{abs}) \cdot canopy_{NIR-abs}) \tag{46}$$

Estimates of incoming short-wave radiation are widely available, however partitioned estimates of NIR and PAR are less frequent. In such circumstances we assume a fixed ratio between PAR and total short-wave radiation ($PAR : SW$).

$$\text{PAR} = \text{SW} \cdot PAR : SW \tag{47}$$

$$\text{NIR} = \text{SW} - \text{PAR} \tag{48}$$

2.7.2 Isothermal long-wave radiation absorption

The long-wave radiation balance is estimated assuming isothermal conditions (i.e. the surfaces are assumed to be the same temperature as the surrounding air). Calculation of the isothermal long-wave radiation is a trade-off between need to account for a positive bias in available energy for evaporation should only the short-wave radiation be accounted for, and errors introduced by not considering thermal heating and cooling of surfaces.

Similar to the short-wave radiative transfer scheme described above ACM-GPP-ET uses a bi-directional radiative transfer scheme the estimate the absorption and emission of long-wave by the canopy and soil surface. The long-wave radiation balance is divided into four components. First, incoming radiation interacts with the canopy either being reflected back toward the sky, transmitted toward the soil surface or absorbed by the canopy. Second, the radiation which is transmitted through the canopy to the soil surface is either absorbed or reflected back through the canopy. Third, the soil surface emits long-wave radiation towards the canopy, repeating step 1 in reverse. Fourth, the canopy itself emits long-wave radiation which is either incident on the soil surface or lost to the sky.

Emission of long-wave radiation (W/m^2) is dependent on temperature and emissivity (σ) related by the Stefan-Boltzmann's constant (κ). Incoming long-wave radiation (LW) from the sky is assumed to be related to surface air temperature (T_{airK}) minus 20 °C, while long-wave emission (LW$_{em}$) from surfaces is assumed to be related to surface air temperature under isothermal conditions.

$$\mathrm{LW} = \sigma \cdot \kappa \cdot (T_{airK} - 20)^4 \tag{49}$$

$$\mathrm{LW}_{em} = \sigma \cdot \kappa \cdot (T_{airK})^4 \tag{50}$$

The fraction of incoming LW to be reflected ($canopy_{LW-refl}$), transmitted ($canopy_{LW-trans}$) and absorbed ($canopy_{LW-abs}$) by the canopy are estimates as a function of LAI.

$$canopy_{LW-refl} = \frac{\alpha_{LW-refl} \cdot \mathrm{LAI}}{\mathrm{LAI} + K_{LW-refl}} \tag{51}$$

$$canopy_{LW-trans} = 1 - \frac{\alpha_{LW-trans} \cdot \mathrm{LAI}}{\mathrm{LAI} + K_{LW-trans}} \tag{52}$$

$$canopy_{LW-abs} = 1 - canopy_{LW-refl} - canopy_{LW-trans} \tag{53}$$

The canopy emits long-wave radiation (=LW$_{em}$·LAI) much of which it absorbed within the canopy itself, resulting in a decreasing fraction of long-wave emitted by the canopy from actually leaving the canopy airspace ($canopy_{LW-release}$).

$$canopy_{LW-release} = 1 - \frac{\alpha_{LW-release} \cdot \mathrm{LAI}}{\mathrm{LAI} + K_{LW-release}} \tag{54}$$

The soil surface also emits long-wave radiation (=LW$_{em}$) which is absorbed, reflected or transmitted through the canopy above. Net absorption of long-wave radiation by the canopy is therefore calculated as

$$ALW_{canopy} = \mathrm{LW} \cdot canopy_{LW-abs} + \mathrm{LW}_{em} \cdot canopy_{LW-abs} - \mathrm{LW}_{em} \cdot \mathrm{LAI} \cdot 2 \cdot canopy_{LW-release} \tag{55}$$

Note the factor 2 refers to the two sides of a leaf both of which are releasing long-wave radiation, one heading upwards towards the sky and the other heading downwards towards the soil. The net absorption of long-wave radiation by the soil is estimated as

$$ALW_{soil} = \sigma \cdot (\mathrm{LW} \cdot canopy_{LW-trans} + \mathrm{LW}_{em} \cdot \mathrm{LAI} \cdot canopy_{LW-release}) - \mathrm{LW}_{em} \tag{56}$$

where absorption of incident long-wave radiation is assumed to be equal to σ. We note a small quantity of long-wave emitted from the soil will be reflected back to the surface, however this is typically < 1 % of the long-wave energy budget and is neglected here.

2.8 Aerodynamic conductance

2.8.1 Canopy aerodynamic conductance

Canopy conductance of water vapour (g$_b$; m/s) and CO$_2$ is estimated using the leaf-level boundary layer conductance model used in SPA (Nikolov et al., 1995; Smallman et al., 2013). We assume that exchange is dominate at the top of the canopy and that conductance should be linked to the canopy top wind speed (u_h; m/s). Note that the boundary layer conductance model allows simulation of both free and forced convection, although here we simulate only the forced convection due to the lack of an explicit simulation of the energy balance. A detailed description of conductance model is given in Nikolov et al. (1995).

$$g_b = \frac{D_{wv} S_h}{d_o} \cdot 0.5 \cdot \mathrm{LAI} \tag{57}$$

where g_b is the conductance for water vapour (m/s), D_{wv} is the temperature dependent molecular diffusivity of water vapour (m^2/s), where D_{wv20} (0.0000242) is D_{wv} at a 20^{o}C (293.15 K) reference temperature. S_h the Sherwood number and d_o is the leaf diameter.

$$D_{wv} = D_{wv20} \cdot \left(\frac{T_{airK}}{293.15}\right)^{1.75} \tag{58}$$

S_h is estimated as a fraction of the Nusselt number (N_u), while N_u is a function of the Prandtl (P_r = 0.72) and Reynolds (R_e) numbers.

$$S_h = 0.962 \cdot N_u \tag{59}$$

$$N_u = 1.18 \cdot P_r^{1/3} \cdot R_e^{1/2} \tag{60}$$

$$R_e = \frac{d_o \cdot u_h}{v} \tag{61}$$

$$v = \frac{\mu}{\rho_{air}} \tag{62}$$

$$\mu = \left(\frac{T_{airK}^{1.5}}{T_{airK} + 120}\right) \cdot 1.4963\mathrm{x}10^{-6} \tag{63}$$

where v is the kinematic viscosity (m^2/s) and μ is the dynamic viscosity (kg/m^2/s).

Above canopy momentum decay follows the standard log law decay assuming neutral conditions (Garratt, 1992).

$$u_h = \frac{u_*}{\kappa} \cdot log\left(\frac{z_h - d}{z_0}\right) \tag{64}$$

where κ is Von Karman constant (0.41), d is the canopy zero plane displacement height (m), z_0 is the canopy roughness length (m) and u_* is the friction velocity (m/s). d and z_0 are calculated based on canopy structure (height z_h and LAI) as described in Raupach (1994).

$$d = z_h\left[1 - \frac{1-\exp(-(C_{d1}\mathrm{LAI})^{0.5})}{(C_{d1}\mathrm{LAI})^{0.5}}\right] \tag{65}$$

and

$$z_0 = \left(1 - \frac{d}{z_h}\right)\exp\left(-\kappa\frac{u_h}{u_*} - \Psi_h\right)z_h, \tag{66}$$

where C_{d1} is an empirically fitted parameter (7.5) and Ψ_h (0.193) corrects the roughness length for the the effect of the roughness sub-layer. u_* is estimated as a function of LAI and u_h

$$u_* = u_h \cdot (C_s + C_r \cdot \mathrm{LAI} \cdot 0.5)^{0.5} \tag{67}$$

where C_s = 0.003 approximates the impact of substrate drag and C_r = 0.3 corrects for the roughness sub-layer (Raupach, 1994).

2.8.2 Soil aerodynamic conductance

Soil aerodynamic conductance (g_{soil}; m s^{-1}) is first calculated as a resistance. Soil resistance is integrated from the soil roughness length (z_{soil} = 0.001 m) through the canopy based on the turbulent eddy diffusivity following Niu and Yang (2004).

$$r_{\mathrm{soil}} = \int_{z_{\mathrm{soil}}}^{d+z_0} dz/K_h(z), \tag{68}$$

where dz is the vertical step size (m) through the canopy and K_h is the eddy diffusivity at z position (m) within the canopy. Eddy diffusivity (K_h; m^2 s^{-1}) is assumed to have an exponential decay through the canopy (as with momentum). Eddy diffusivity at the canopy top is estimated as specified in Kaimal and Finnigan (1994).

$$K_h(z_h) = \kappa u_*(z_h - d) \tag{69}$$

K_h is decayed through the canopy as described below.

$$K_h(z) = K_h(z_h)\exp(-f(1 - z/z_h)) \tag{70}$$

$$f = (c_d z_h \mathrm{LAI}/l_m)^{0.5}(\Phi_m)^{0.5} \tag{71}$$

The coefficient of momentum decay f is dependent on c_d the coefficient of drag for foliage (0.2), LAI, l_m and soil surface Monin-Obukov similarity coefficient (Φ_m). Φ_m is assumed to be = 1 describing neutral conditions Garratt (1992).

2.9 Plant hydraulic resistance

We use a mechanistic model of plant hydraulics to determine the maximum available water supply to the canopy from each of the three potential rooting layers (E$_{layer}$; mmolH$_2$0/m^2/s) under steady state flow (Jones, 1992). The advantage to using a mechanistic approach allows for the estimation of physiological properties which makes possible novel comparisons with field observations such as Poyatos et al. (2016). The model assumes that the canopy is at LWP_{min} drawing from each of the three soil layers based on their layer specific SWP, canopy, root and soil hydraulic resistances (MPa/s/m^2/mmol).

$$\mathrm{E}_{layer} = \frac{|LWP_{min} - \mathrm{SWP}| + (\rho_{lw} \cdot g \cdot z_h)}{\mathrm{R}_{soil} + \mathrm{R}_{root} + \mathrm{R}_{canopy}} \tag{72}$$

Where ρ_{lw} is the density of liquid water (1000 kg/m^3) and g is the acceleration of gravity (9.82 m/s^2). The hydraulic resistance due to the soil (R$_{soil}$), roots (R$_{root}$) and the combined resistance of the stem and branch (R$_{canopy}$) each have units of MPa/s/m^2/mmol.

$$\mathrm{R}_{soil} = \frac{ln(r_s/Root_{radius})}{2 \cdot \pi \cdot l_R \cdot l_s \cdot G_s} \tag{73}$$

$$\mathrm{R}_{root} = \frac{Root_{resist}}{\mathrm{C}_{root} \cdot 2 \cdot l_s} \tag{74}$$

$$\mathrm{R}_{canopy} = \frac{z_h}{G_p \cdot \mathrm{LAI}} \tag{75}$$

$Root_{radius}$ is the mean root radius (0.00029 m Bonan et al., 2014) and r_s is the mean distance between roots (m). l_R is the root length (m) within the current soil layer and l_s is the thickness of the current soil layer (m). $Root_{resist}$ is the root resistivity (25 MPa/s/g/mmolH$_2$0; Bonan et al., 2014), G_p is the plant conductivity to water (5 mmolH$_2$O/m$_{leafarea}$/s/MPa; Bonan et al., 2014).

$$r_s = \frac{1}{(l_R \cdot \pi)^{0.5}} \tag{76}$$

The root length (l_R) within each of the three soil layers available for root access is a function of available root biomass within that layer (Root$_{layer}$; g/m^2). The total root biomass (Root$_{total}$; g/m^2) is distributed between the three soil layers assuming that 50 % of the biomass is in the top 25 % of the rooting profile. Where the current rooting depth ($D_{root-cur}$; m) is assumed to follow an exponentially decaying function.

$$I_R = \frac{\mathrm{Root}_{layer}}{Root_{density} \cdot pi \cdot Root^2_{radius}} \tag{77}$$

$$D_{root_cur} = \frac{Root_{max} \cdot \mathrm{Root}_{total}}{K_{root} + \mathrm{Root}_{total}} \tag{78}$$

G_s is the soil conductivity (m^2/s/MPa) which is calculated as a function of soil textural parameters derived from the Saxton model of soil hydraulics (sax_{c1}, sax_{c2} and sax_{c3}) and volumetric water content (Θ; m^3/m^3). For further details see Saxton et al. (1986); Williams et al. (2001b)

$$G_s = sax_{c1} \cdot e^{\frac{sax_{c2} + sax_{c3}}{\Theta}} \tag{79}$$

The ratio of E$_{layer}$/ΣE$_{layer}$ determines the proportional extraction of water from each soil layer (Up_{frac}) due to E$_{trans}$.

$$Up_{frac} = \frac{E_{layer}}{\Sigma E_{layer}} \tag{80}$$

For use else where in the model the soil layer specific SWP and hydraulic resistances are aggregated based on uptake potential from each soil layer to provide an apparent SWP and resistance, i.e. the weighted soil water potential (wSWP) and total hydraulic resistance (R$_{tot}$).

$$\text{wSWP} = \Sigma(\text{SWP} \cdot Up_{frac}) \tag{81}$$

$$\text{R}_{tot} = \frac{\Sigma|LWP_{min} - \text{wSWP}|}{\Sigma E_{layer}} \tag{82}$$

2.10 Soil water balance

The Saxton model of soil hydraulics is used as the basis for simulation of the soil water balance within ACM-GPP-ET (Saxton et al., 1986). The implementation is a simplified version of that used within the SPA model (Williams et al., 2001b; Smallman et al., 2013). A total of four soil layers are simulated by the model, three of these layers are available for root access depending on the amount of root currently available. The first soil-layer has a fixed depth of 10 cm from which soil surface evaporation is extracted, while the second-layer has a fixed depth of 20 cm (i.e. total depth of first and second soil layers is 30 cm). The third layer has a variable depth dependent on the penetration depth of the roots within this layer (i.e. root biomass), thus providing a potential advantage of increasing rooting depth to access water resources deeper within the soil. The fourth soil layer is defined by the maximum soil rooting depth ($D_{root_{max}}$; m). The soil water mass balance is updated through four stages briefly described below.

The soil water mass balance is updated in sequence dealing will (i) evaporative losses, (ii) gravitational drainage, (iii) infiltration of precipitation and (iv) adjustments to the soil layers based on changes in rooting depth. Evaporative losses from the soil surface are extracted solely from the top soil layer, while water losses due to transpiration are extracted based on the Up_{frac} as determined based on the rooting distribution. The gravitational drainage and infiltration schemes are a simplified implementation of those used by the SPA model (Williams et al., 2001b). Gravitational drainage is then calculated based on the downward flow of water from soil layers currently above their field capacity to deeper layers and ultimately out of the bottom of the soil water column (i.e. drainage flux). Precipitation which reaches the soil surface infiltrates based on the available pore space (i.e. porosity) of the soil layers. As the minimum time period used for the model is daily we assume that the maximum available pore space can be utilised. Once all soil layers have filled all available pore space (i.e. the soil is saturated) all remaining precipitation is assumed to be lost from the system as run-off.

3 Calibration procedure

We used the Soil Plant Atmosphere (SPA, Williams et al., 1996; Smallman et al., 2013) model to generate a data set of photosynthetic and evaporative fluxes for the calibration of ACM-GPP-ET. The calibration of ACM-GPP-ET was conducted using the CARDAMOM model-data fusion framework (Bloom and Williams , 2015). SPA simulated a 12 year period (2001-2012) at an hourly time step for 200 locations selected using a stratified random process from across the global land surface (Figure 2); stratification was to ensure even coverage across the latitudinal gradient. The number of sites selected was a trade-off to ensure good spatial coverage of training data but to end with a calibration dataset comprised of $\sim$50,000 days to reduce computational cost for the calibration process. Land cover areas covered by desert, rocky areas or dominated by C4 photosynthetic pathway vegetation, as specified in the ECMWF land cover map, were excluded from the sampling to avoid areas which do not have substantial photosynthetic activity and to reflect the fact that ACM-GPP-ET is designed to simulate the dominant C3 photosynthetic pathway. ~~Soil sand and clay contents were extracted from the Harmonized World Soils Database (HWSD; Heiderer and Kochy, 2011), locations for which the sand / clay content fall outside the parameterised bounds for the Saxton soil hydrological model were also excluded ($\sim$0.7 % of global land surface).~~ ~~For the generation of the calibration dataset SPA's soil water content was held at field capacity allowing all hydraulic variation to be dependent on root biomass and penetration of the soil profile. The SPA simulations were repeated a second time at the calibration sites but allowing soil water content to vary to provide a validation dataset to assess the ability of ACM-GPP-ET to simulate the impacts of varied plant water availability.~~ To isolate the impact of root biomass and vertical distribution on water supply from the role soil moisture status SPA's soil moisture is held at field capacity for the creation of the calibration dataset. However. part of the validation process (See section 4 for details) SPA is re-run but this time allowing the soil moisture status to vary in response to inputs and losses to facilitate validation of ACM-GPP-ET's capacity to simulate the development of drought compared to our complex model.

For both the calibration and validation simulations SPA (and ACM-GPP-ET) require inputs of meteorological drivers, foliar nitrogen, soil textural information and timeseries of LAI and root biomass. Prescribing LAI and root biomass, opposed to coupling ACM-GPP-ET to a C-cycle model, allows the isolation of photosynthetic driver sensitivity without complex C-cycle feedbacks. Meteorological drivers were taken from the ERA-Interim reanalysis (Dee et al., 2011), these drivers were downscaled to an hourly time step using a weather generator (https://github.com/GCEL/WeatherGenerator_v1). Atmospheric CO$_2$ concentration ~~was linearly increased from 300 ppm in 2001 to 450 ppm in 2012,~~for each day was sampled from 300-450 ppm; the exaggerated CO$_2$ range is to ensure that influence of increasing CO$_2$ concentrations is contained within the calibration dataset. Note that prescribing LAI, root biomass and fixing soil moisture at field capacity prevents propagation of unexpected / undesired responses to strongly increasing atmospheric CO$_2$ gradients, i.e. each day's GPP and ET are purely as a function of that day's conditions. Mean foliar nitrogen content was randomly sampled for each site (but held constant over time) from log10 normal distribution (mean = 1.89 gN/m^2; Kattge et al., 2011). Soil sand and clay contents were extracted from the Harmonized World Soils Database (HWSD; Hiederer and Köchy, 2011), locations for which the sand / clay content fall outside the parameterised bounds for the Saxton soil hydrological model were also excluded ($\sim$0.7 % of global land surface). Timeseries of LAI and root stocks used to driver SPA and ACM-GPP-ET were extracted from a global terrestrial carbon cycle mode-data fusion analysis (Bloom et al., 2016). ~~which used a simplified version of the SPA model, DALEC (Williams et al., 2005, Fox et al., 2009, Smallman et al., 2007), and the ACM-GPP model (Williams et al.,1997). The CARDAMOM analysis assimilated MODIS LAI and tropical above ground biomass estimates resulting in a continuous time series of LAI, while root stocks are generated through a mass balance system which respects ecological realism (Bloom and Williams 2015) as well as the information fed into the analysis~~We used LAI and fine roots datasets from Bloom et al. (2016) derived from

MODIS LAI products, remotely sensed above ground biomass and ecological process knowledge (for details see Bloom and Williams , 2015).

In order to quantify the ability of the analysis framework to retrieve accurate ecophysiological trait information (e.g. optimum temperature of photosynthesis) a single set of ecophysiological parameters are used to drive SPA. This nominal parameter set are a combination of the forest hydraulic parameters from Williams et al. (1996) and broad-leaf forest radiation reflectance parameters Smallman et al. (2013).

The hourly SPA simulations were aggregated to daily time step and then sub-sampled at a 2-weekly interval to reduce temporal auto-correlation. Further filtering was applied to remove days with zero GPP (i.e. winter) and days for which SPA was unable to solve its energy balance closure to a cumulative absolute error, over sub-daily time steps, of less than 50 W/m^2 summed across each 24-hour period. Thus, after filtering some 42,658 simulation days available for calibration.

3.1 SPA

The Soil Plant Atmosphere (SPA; Williams et al., 1996; Smallman et al., 2013) model simulates a mechanistic representation of the terrestrial ecosystem, coupling plant carbon and water cycles through ecophysiological principles. SPA simulates up to 10 canopy layers simulating both sunlit and shaded leaf area; each being independently connected to water supply from the soil. Water accessibility from 20 soil layers is determined as a function of root penetration within each soil layer. SPA estimates the surface exchanges of heat, water and CO_2 within a mass and energy balanced framework. SPA has been extensively validated at range of spatial scales (leaf to landscape) and climate zones (tropical, temperate and Arctic) (Williams et al., 1998, 2001b; Fisher et al., 2006, 2007; Sus et al., 2010; Smallman et al., 2013, 2014; López-Blanco et al., 2018). A detailed description of SPA and its major developments can be found in Williams et al. (1996, 1998, 2001b, 2005); Sus et al. (2010); Smallman et al. (2013), however a brief description follows below.

Leaf level photosynthesis (Farquhar; Farquhar and von Caemmerer, 1982), transpiration (Penman-Monteith; Jones, 1992) and energy balance are coupled via a mechanistic model of stomatal conductance (Williams et al., 1996; Bonan et al., 2014). Stomatal opening is modulated to optimise photosynthetic uptake within constraints determined by (i) the intrinsic water use efficiency and (ii) balancing atmospheric demand with available water supply from the soil. SPA makes use of a detailed multi-canopy layer radiative transfer scheme estimating the absorption and reflectance of both short- and long-wave radiation for the sunlit and shaded leaf area (Williams et al., 1998). Aerodynamic exchange coefficients for water, heat and CO_2 are estimated accounting for above, within and under-canopy momentum decay, including stability corrections based on Monin-Obukov stability theorem (Smallman et al., 2013).

3.2 CARDAMOM

The CARbon DAta MOdel fraMework (CARDAMOM; Bloom and Williams , 2015) is a model-data fusion (MDF) framework. CARDAMOM uses a Bayesian approach within a Metropolis Hastings - Markov Chain Monte Carlo (MH-MCMC) algorithm to retrieve parameters for a given model as a function of observational constraints. Parameter priors are specified with a uniform probability distribution truncated between minimum and maximum values (Table 1). ~~In this study CARDAMOM retrieved parameters~~

~~for the DALEC terrestrial carbon cycle model to generate time series of LAI and root biomass for the calibration (2001-2012) and validation (2001-2015) procedure (Bloom et al., 2016, Smallman et al., 2017). CARDAMOM is also used to conduct the calibration of ACM-GPP-ET.~~ CARDAMOM was used to calibrate ACM-GPP-ET based on GPP, transpiration, soil evaporation and evaporation of intercepted rainfall provided by SPA.

~~Here the SPA model provides GPP and evaporative fluxes against which the parameters for ACM-GPP-ET are optimised.~~ For the purpose of calculating the cost function used within the MDF approach we assumed uncertainties consistent with those expected from Eddy covariance. The uncertainty of both GPP and evaporative fluxes are assumed to be 15 %, representing random error estimates typically found for Eddy covariance (Stoy et al., 2006; Mauder et al., 2013). The use of the SPA model with known input parameters allows for quantification of how accurately the equivalent retrieved parameters have been determined. Where there is a directly equivalent parameter between SPA and ACM-GPP-ET the SPA values are provided in Table 1.

4 Validation procedure

ACM-GPP-ET is validated over two phases using a range of evapo-transpiration and GPP estimates from ~~both~~1) out-of-sample SPA simulations and 2) fully independent eddy covariance derived estimates from the FLUXNET2015 database.

4.1 SPA validation

~~Phase 1) comparison against out-of-sample SPA simulated estimates of GPP and evapo-transpiration.~~Phase 1) tests the ability of ACM-GPP-ET to simulate the soil moisture dynamics and resulting feedbacks on plant photosynthesis and evaporation estimated by the state-of-the-art SPA model. To achieve this we compare out-of-sample SPA simulated estimates of GPP and evapotranspiration. SPA's soil moisture status was held constant at field capacity during calibration phase and substantially sub-sampled. Here SPA's soil moisture status was allowed to vary as a function of its inputs and outputs, these simulations were carried out at the same locations as those used for the calibration analysis but without any sub-sampling. ~~These SPA simulations tests the ability of ACM-GPP-ET to simulate the soil moisture dynamics and resulting feedbacks on plant photosynthesis and evaporation.~~

4.2 Independent validation: FLUXNET2015

Phase 2) quantifies ACM-GPP-ET's predictive skill using fully independent observations. Furthermore, we contrast ACM-GPP-ET's predictive capacity with that of SPA. To achieve this comparison, both ACM-GPP-ET and SPA are simulated carbon and water fluxes at FLUXNET 2015 sites.~~Phase 2) uses fully independent observations to provide validation of ACM-GPP-ET's predictive skill but also to determine the consistency of predictive capability between our model of intermediate complexity and that of our highly complex model.~~ This is achieved by both ACM-GPP-ET and SPA simulating carbon and water fluxes at FLUXNET2015 sites. The SPA simulations use the same nominal set of ecophysiological parameters used in generating the calibration dataset. ACM-GPP-ET uses the maximum likelihood parameter set retrieved during the calibration procedure. The parameter set used here broadly represent a forest ecosystem.~~, therefore we expect that both SPA and ACM-GPP-ET will perform best at forest sites and less well at sites with different hydraulic~~

~~traits.~~Therefore, we hypothesise that both SPA and ACM-GPP-ET will perform best at forest sites and less well at sites with different hydraulic traits.

Daily estimates of GPP and ET derived from Eddy covariance were extracted from the FLUXNET2015 database (http://fluxnet.fluxdata.org/, accessed 01/11/2016). The FLUXNET2015 database was filtered to include only sites which overlapped our simulation period (2001-2015) for a minimum of three years, to allow for inter-annual comparison, and not more than 20 % missing data. ACM-GPP-ET is designed to emulate the C3 photosynthetic pathway, therefore sites which are listed to be dominated by vegetation which use the C4 or CAM pathways were removed. We also removed estimates which do not carry the highest quality flags to avoid comparing our model against estimates generates using a statistical model of net exchange (i.e. we use only the non-gap filled observations). Eddy covariance estimates where energy balance non-closure is less than 85 % were also rejected. In total 497 site years encompassing 10 vegetation types across 59 sites were available for validation of GPP and ET. Meteorological drivers used to driver SPA and ACM-GPP-ET were extracted from the the local site level measurements. Missing data were gap-filled either assuming linear interpretation (for single missing hours) or extracted from bias corrected temporally down-scaled meteorological drivers as used in the calibration process. Finally, as with the earlier SPA simulations LAI and root biomass for each site are extracted from Bloom et al. (2016). ~~ACM-GPP-ET is dependent on inputs of LAI, fine root stocks and parameters defining rooting depth. Such information is available only for a small number of field sites and typically lacking the temporal consistency required for our simulations. Here the LAI and fine root stocks are extracted from the global 1 x 1 degree CARDAMOM analysis (Bloom et al., 2016) used as part of the calibration procedure (see above).~~

5 Results

We show that a single global calibration of ACM-GPP-ET can effectively reproduce the patterns of GPP and ET simulated by SPA. Importantly the predictions of WUE are consistent for both ACM-GPP-ET and SPA, so that the simplified model is able to capture the interactions between C and water cycling. We also describe an independent validation against FLUXNET data, across 59 sites.

5.1 SPA calibration / validation

A single global ACM-GPP-ET parameterisation simulates the calibration dataset with a high degree of skill when using the maximum-likelihood parameter sets retrieved from the calibration analysis (Figure 3). The dynamics of soil evaporation is best simulated by ACM-GPP-ET followed by GPP and transpiration, each achieving R^2 $\geq$0.91. Evaporation of canopy intercepted precipitation achieved a lower R^2 at 0.81. All fluxes are largely unbiased (GPP bias = -0.2gC/m^2/day and evaporative fluxes magnitude $\leq$0.08 kgH$_2$O/m^2/day) with low RMSE (0.97 gC/m^2/day and $\leq$0.39 kgH$_2$O/m^2/day). However, we note a tendency to underestimate peaks in transpiration found in the SPA simulation (Figure 3). Evaporation of canopy intercepted precipitation is least well simulated by each metric used here; however this is expected given the sensitivity of this flux to the timing and intensity of precipitation events and canopy energy balance varying strongly at a sub-daily time scales which are not accounted for here. Transpiration (E_{trans}; 61 %) dominates the overall ACM-GPP-ET simulated evaporative budget followed by evaporation of canopy intercepted rainfall (E_{wet}; 34 %) and soil surface evaporation (E_{soil}; 5 %), broadly consistent with those simulated by SPA in the calibration dataset (67 %, 28 % and 5 % respectively). ACM-GPP-ET is 2200 times faster than SPA, where ACM-GPP-ET requires ∼0.000007 seconds per day and SPA 0.015 seconds per day. Overall, ACM-GPP-ET simulates the calibration dataset with substantial skill and a substantial reduction in computational requirements.

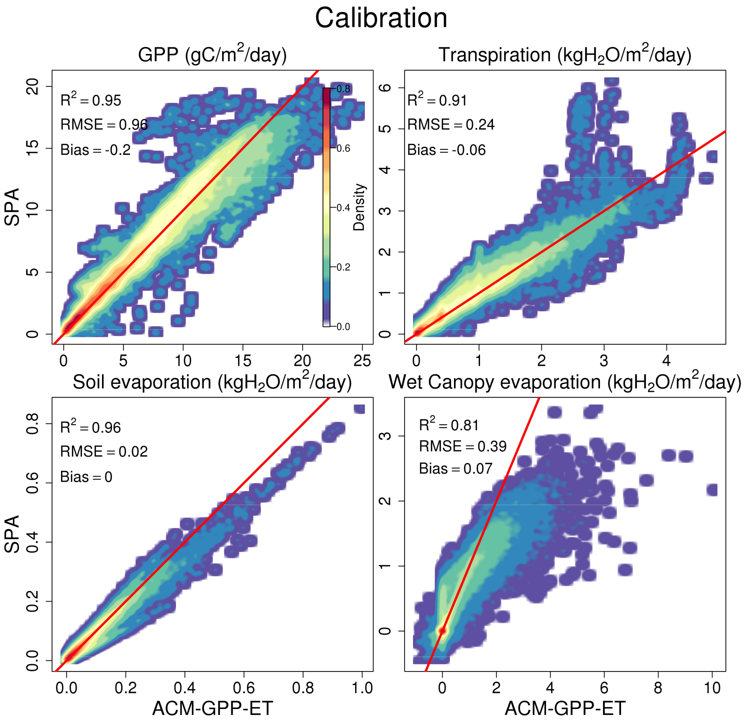

Figure 3. Comparison between SPA and ACM-GPP-ET generated fluxes, where ACM-GPP-ET used the maximum likelihood parameter sets for the calibration procedure. Fluxes compared are gross primary productivity (gC/m^2/day), transpiration (kgH_2O/m^2/day), soil evaporation (kgH_2O/m^2/day) and evaporation of water intercepted by the canopy (kgH_2O/m^2/day). The red line is a 1:1 line for reference. The colour intensity from blue to red indicates the density of flux estimates within a given area, note that for clarify showing low density areas the density values are scaled by density$^{1/4}$.

~~ACM-GPP-ET's~~ Simulation of carbon and water fluxes remains robust in the phase 1) validation where ACM-GPP-ET is ~~when~~compared against the out-of-sample SPA simulations were soil moisture content is dynamically simulated, i.e. not held at field capacity as in the calibration procedure (Figure 4). Similarly, partitioning between evaporative fluxes remains closely aligned between ACM-GPP-ET (E_{trans} = 59 %, E_{wet} = 35 %, E_{soil} = 6 %) and SPA (E_{trans} = 62 %, E_{wet} = 35 %, E_{soil} = 7 %). Only soil evaporation suffers a substantial reduction in the simulation of the variability of SPA's soil evaporation from R^2 = 0.96 to 0.59, however remaining unbiased and RMSE increasing by only 0.02 kgH_2O/m^2/day (Figure 4).

Ecosystem water use efficiency (WUE = GPP / E_{trans}) simulated by SPA is well predicted by ACM-GPP-ET (R^2 = 0.79, RMSE = 1.88 gC/kgH_2O, bias = 0.33 gC/kgH_2O). The consistency within simulations with dynamic water availability demonstrates resilience in ACM-GPP-ET's ability to represent the linkages between the plant carbon and water cycles, which is key when considering the impacts of climatic extremes such as the evolution of drought. This ability to simulate drought in a manor consistent with SPA is supported by the high quality simulation of soil moisture content (R^2 = 0.84, RMSE = 4.19 kgH_2O/m^2, bias = 1.17 kgH_2O/m^2; Figure 4).

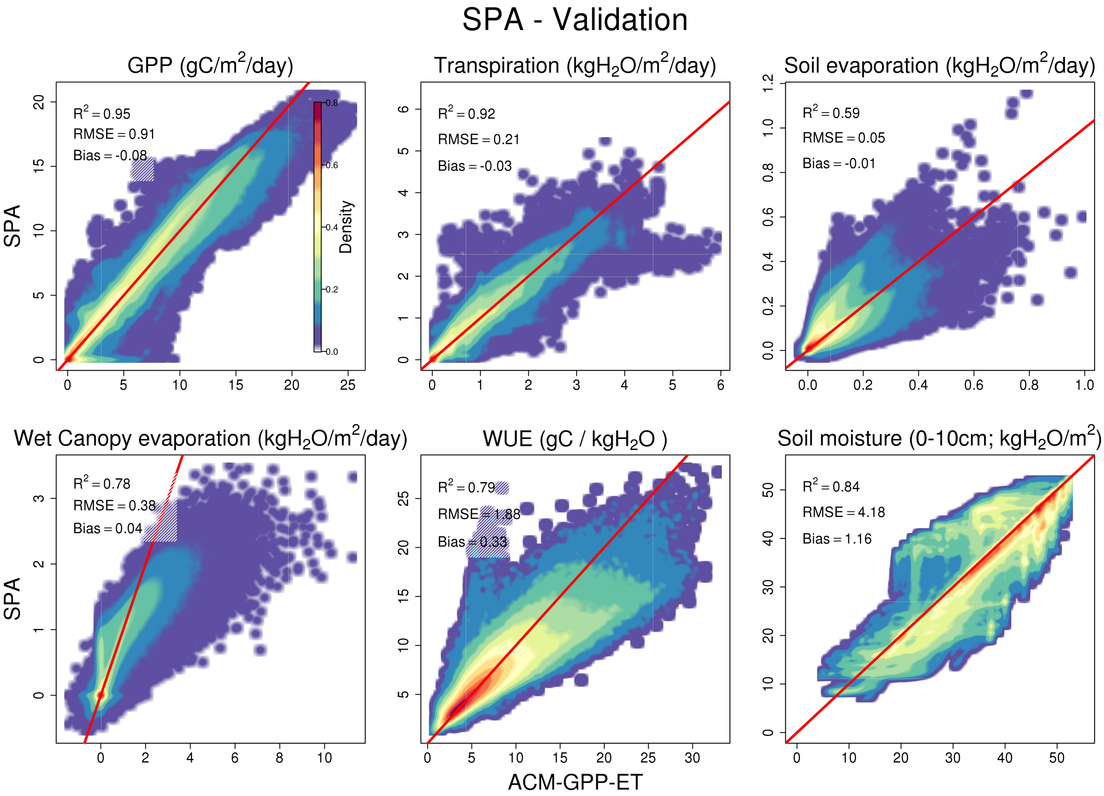

Figure 4. Comparison between ACM-GPP-ET and SPA simulated fluxes for model based validation of ACM-GPP-ET's ability to simulate coupled plant carbon and water cycle dynamics. ACM-GPP-ET uses the maximum likelihood parameter set from the calibration procedure. Fluxes compared are gross primary productivity (gC/m^2/day), transpiration (kgH_2O/m^2/day), soil evaporation (kgH_2O/m^2/day) and evaporation of water intercepted by the canopy (kgH_2O/m^2/day). Also shown is the soil moisture content in the 0-10 cm soil layer (kgH_2O/m^2) and water use efficiency (WUE = GPP / T; gC/kgH_2O). The red line is a 1:1 line for reference. The colour intensity from blue to red indicates the density of flux estimates within a given area, note that for clarify showing low density areas the density values are scaled by density$^{1/4}$.

Table 4. Summary statistics for the global comparison between GPP and ET estimated by both ACM-GPP-ET, SPA and the FLUXNET2015 database. Statistics include R^2, root mean square error (RMSE) and mean bias (model-obs), GPP units are gC/m$_2$/day and ET are in units of kgH$_2$O/m^2/day.

Model	Flux	R^2	RMSE	Bias
SPA	GPP	0.59	2.57	-0.81
	ET	0.48	1.23	-0.90
ACM-GPP-ET	GPP	0.61	2.41	-0.66
	ET	0.58	1.07	-0.77

5.2 FLUXNET2015: Independent validation

For phase 2) validation ACM-GPP-ET and SPA simulated GPP and ET estimates for 59 sites from the FLUXNET2015 database to provide fully independent validation of ACM-GPP-ET's ability to simulate real-world estimates but also of its predictive skill compared to that of SPA (Table 4; Figure 5). For the FLUXNET validation we aim to achieve a similar degree of predictive capacity to existing remote sensing driven estimates. As stated earlier we hypothese that both ACM-GPP-ET and SPA will perform better at forest sites than in other ecosystems. GPP is typically better predicted than ET by both ACM-GPP-ET and SPA, which is expected given that ET is the combination of three evaporative fluxes (ET = E_{trans} + E_{wet} + E_{soil}). Both GPP and ET are underestimated by ACM-GPP-ET and SPA with larger RMSEs than found when comparing between ACM-GPP-ET and SPA simulations (Table 4). However, ACM-GPP-ET marginally out-performs SPA at most sites and for ET in particular. The between site distribution of R^2 and RMSE is skewed with a relatively small number of sites performing poorly (Figure 5). For each metric shown (R^2, RMSE and bias) the distribution achieved by ACM-GPP-ET indicates a potentially greater degree of predictive skill at daily time step than SPA.

ACM-GPP-ET and SPA perform well at forested sites (except evergreen broad-leaf forests), with more variable performance at grassland, crop and savannah type ecosystems (Figure 6). However, both ACM-GPP-ET and SPA demonstrated a clear capability to simulate inter-site variation (i.e. the mean GPP and/or ET between sites) R^2 $\sim$0.94 for both GPP and ET. Variation in predictive capability is not unexpected given that we use a single set of parameters for both models without site specific modifications~~(except the use of location specific meteorology and LAI)~~.

ACM-GPP-ET simulated and Eddy covariance derived estimates of GPP and ET were compared at different temporal aggregations (weekly, monthly and annual) showing good skill at simulating seasonal and inter-annual dynamics. From daily through to weekly and monthly aggregation the statistical agreement between variation in simulated and observed estimated improves considerably. Estimation of ET is most improved increasing from R^2 = 0.58 $\rightarrow$ 0.72 $\rightarrow$ 0.75 while for GPP R^2 increases from 0.61 $\rightarrow$ 0.65 $\rightarrow$ 0.68. RMSE and mean bias remain largely unchanged. However, simulation of inter-annual variation is more challenging with the R^2 for GPP = 0.68 and ET = 0.46. A similar pattern of results is found for SPA (not shown).

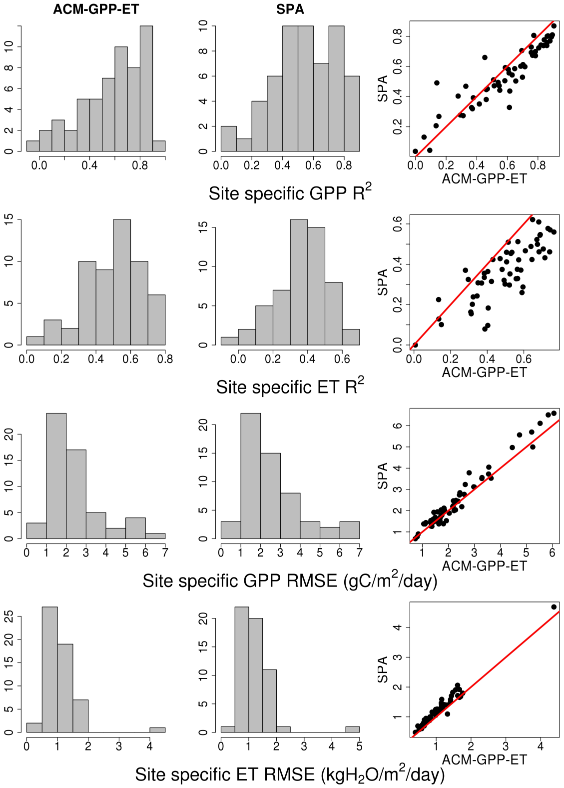

Figure 5. Comparison of ACM-GPP-ET and SPA simulating fully independent gross primary productivity (GPP) and evapotranspiration (ET) from FLUXNET2015. The histograms show the site specific R^2 and RMSE. SPA is shown in the left column, ACM-GPP-ET is in the centre. In the right column shows the site by site comparison of statistical metrics achieved by each model.

6 Discussion

In this study we have described, calibrated (Figure 3) and validated (Figure 4-7) a model of intermediate complexity, the Aggregated Canopy Model for Gross Primary Productivity and Evapo-Transpiration (ACM-GPP-ET v1). ~~ACM-GPP-ET is $\sim$2200 times faster than SPA, requiring just 0.000007 seconds per time step, rendering it practicable for large ensemble analyses. Our profiling of the model code (not shown) highlights several challenge in representing complex non-linear processes in a simple computationally efficient manor while maintaining predictive skill. ACM-GPP-ET provides a computationally efficient representation of plant photosynthesis and water cycle, coupled through process-orientated ecophysiological principles (Figure 1)~~ACM-GPP-ET provides a process orientated representation of plant photosynthesis and water cycle, coupled through ecophysiological principles (Figure 1). ACM-GPP-ET simulations using a single global calibration have been validated against simulated GPP and evaporative fluxes but also emergent properties including WUE and soil moisture status from the state-of-the-art SPA model. These simulations were driven with LAI, fine root stock and meteorological

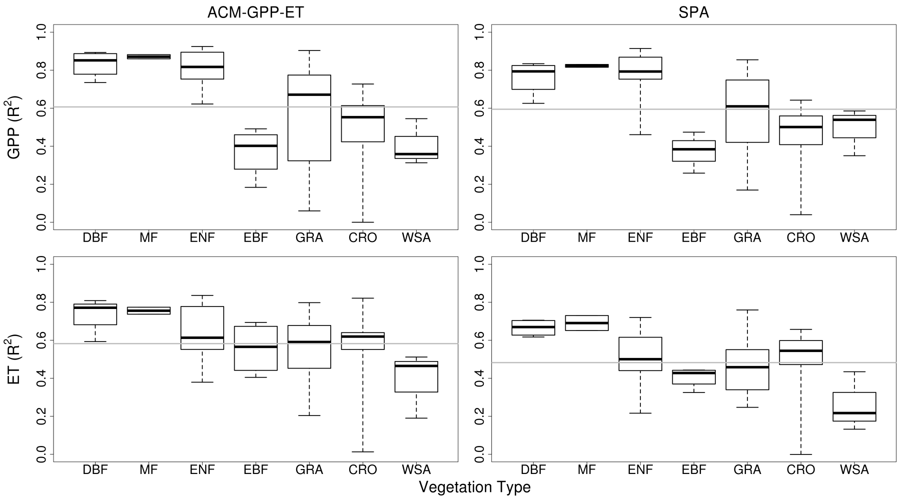

Figure 6. Independent validation of ACM-GPP-ET and SPA using eddy covariance derived estimates of gross primary productivity (GPP) and evapotranspiration (ET) from the FLUXNET2015. Box and whisker plots show the site specific R^2 values for each of the International Geosphere-Biosphere Programme (IGBP) vegetation classification. CRO = cropland, CSH = closed canopy shrubland, DBF = deciduous broad-leaf forest, EBF = evergreen broad-leaf forest, ENF = evergreen needle-leaf, GRA = grassland, MF = mixed forest, WSA = woody savanna. The mean for each vegetation classification is shown by the thick centre line, the box represents the 25 % and 75 % quantiles while the whiskers indicate the minimum and maximum values. The horizontal grey line indicates the mean R^2 across groups.

conditions spanning across global gradients (Figure 2). Furthermore, to provide fully independent validation we have compared our estimated GPP and ET fluxes, again using a single global calibration, against multiple eddy-covariance-derived flux data from the FLUXNET2015 database, demonstrating substantial predictive skill.

6.1 ~~Computationally efficiency of ACM-GPP-ET~~ACM-GPP-ET: lessons learned on model simplification

~~ACM-GPP-ET is $\sim$2200 times faster than SPA, requiring just 0.000007 seconds per time step, rendering it practicable for large ensemble analyses. Our profiling of the model code (not shown) highlights several challenge in representing complex non-linear processes in a simple computationally efficient manor while maintaining predictive skill.~~ A number of alternate model structures were tested over the course of the development of ACM-GPP-ET, and while it is out of scope to describe these in detail, there are a range of important lessons learned from development of specific components. The single most computationally expensive component is the iterative solution linking photosynthesis and transpiration via stomatal conductance. However, a coupled representation of stomatal conductance linking these processes was essential for maintaining predictive capacity of both canopy exchanges and emergent properties of WUE and soil moisture status. Similarly, the simulation of soil moisture dynamics ~~at daily time step~~is time-consuming, due to the need for simulating non-linear drainage processes occurring at sub-daily time steps. Originally a single layer bucket was tested but was unable to generate reasonable soil moisture dynamics and ultimately drought responses compared with SPA. Our experience is consistent with other studies which have explicitly considered the impact of varying the number of soil moisture layers (Blyth and Daamen , 1997). Water drainage between soil layers and runoff of water from the canopy surface places an upper limit on efficiency achievable while maintaining predictive skill for soil moisture status and indirectly canopy fluxes. However, we expect further efficiency improvements to be achievable through subsequent code modifications including alternate theoretical approaches to achieve the photosynthesis-transpiration coupling. A dedicated focus on code optimality is out of scope for the current study, but is critical to the ongoing process of model improvement.

In this study 22 parameters are calibrated (Table 3), 15 of these are related to the estimation of canopy and / or soil absorption of PAR, NIR and longwave radiation. The key challenge for the radiative transfer was the essential requirement to reproduce the emergent non-linear functional shape between LAI and canopy radiation absorption, transmittance to soil and reflectance making the complex vertical structure implicit in the calibration. We found an appropriate simulation of non-linear radiative transfer was critical for realistic radiative responses of each component of evaporation. In contrast, for a GPP model alone a far simpler radiative transfer scheme was viable(Williams et al., 1997). However, the large number of parameters in the radiative transfer scheme is open to constraint through e.g. remote sensing observations of canopy structure and reflectance. These observations could be used to calibrate the scheme for individual locations but also canopy structural forms (i.e. canopy vertical structure).

6.2 Intermediate complexity emulation of a complex TEM

ACM-GPP-ET accurately simulates its calibration data-set (Figure 3) and out-of-sample validation (Figure 4) generated by the SPA model. Substantial predictive skill was achieved for photosynthesis and each of the evaporative fluxes, but also the unbiased simulation of soil moisture and WUE which were not part of the calibration process (Figure 4). The single global calibration effectively spans global process sensitivity to climate across gradients of latitude, maritime-continental gradients, and seasonal cycles. The calibration also represents the effect of ecological variation of LAI and fine root stocks. By including 10 different drivers we generated a major challenge for model simplification. ACM-GPP-ET must robustly represent functional forms for C and water cycling across these multiple response dimensions, including any interactions. We note an underestimate in peak transpiration fluxes (Figure 3) which we hypothesise is due to the lack of including the impact of energy balance on canopy and non-linear responses at sub-daily timescales. While this bias may in some cases lead to an underestimate of within day drought / water supply limitation ~~T~~the statistical analyses for validation ~~show~~indicate that the functional forms embedded in ACM-GPP-ET effectively represent those arising from complex mechanistic interactions within SPA. ACM-GPP-ET generates robust daily aggregations from SPA's hourly resolution.

ACM-GPP-ET effectively reproduces the eco-climatological sensitivity of plant water use efficiency from the SPA model (Figure 4). Reliable simulation of the dynamics and magnitude of plant WUE is an important property for robust modelling of hydrological, ecological and biological interactions. For climate sensitivity studies, ecosystem carbon-water coupling controls drought development and its interactions with ecosystem processes (Beer et al., 2009; Keenan et al., 2013; Bonan et al., 2014). Similarly, appropriate partitioning of evaporative fluxes, i.e. T/ET, is essential to simulate correctly the overall ecosystem response to change in climate. Transpiration has a direct interaction with biogeochemical cycling through canopy conductance, whereas evaporative fluxes have an indirect effect through adjustments to soil moisture and radiation environment mediated through variation in canopy cover. T/ET estimated by ACM-GPP-ET and SPA are closely aligned for both the calibration procedure with fixed soil moisture and that with dynamic soil moisture. The fraction of T/ET declined under dynamic soil moisture in both models, indicating consistent response to varied water status. This consistency indicates that ACM-GPP-ET effectively represents and aggregates to canopy scale the critical nexus for carbon and water cycling simulated in the leaf-scale stomatal conductance routines of SPA. As noted in section 6.1 alternate coupling approaches could be investigated reduce the computational requirements, but perhaps more importantly our framework allows for the testing of alternate coupling hypotheses to robustly assess their predictive capacity against emergent properties~~Further experiments (not shown) indicate that independent calibration of separate GPP and ET models to SPA outputs fails to produce consistent WUE - joint calibration is critical for success.~~ ~~Moreover~~For example, recent analyses estimate transpiration is responsible for ∼58 % of global evaporation, consistent with both SPA and ACM-GPP-ET estimates, and contrasting with many TEMs which tend to underestimate T/ET partitioning (Wei et al., 2017) but also expanding on the stomatal model comparison conducted by Bonan et al. (2014).

6.3 Comparison to independent flux observations worldwide

A key component of our validation process was the comparison of ACM-GPP-ET and SPA simulated GPP and ET fluxes at 59 FLUXNET2015 sites. We aimed to achieve a comparable predictive skill compared to analyses driven by remotely sensed information. Moreover, we hypothesised that both ACM-GPP-ET and SPA would perform best at forest sites due to the choice of forest based parameters used in the calibration procedure. ACM-GPP-ET and SPA simulated both GPP and ET fluxes with substantial skill, especially given that only a single global parameterisation was used (Table 4; Figure 5-6). Indeed, ACM-GPP-ET slightly out-performs SPA in each statistical metric presented here; the greatest difference is found for simulating daily variation of GPP and in particular ET fluxes (Figure 5). However, it is unlikely that ACM-GPP-ET has actually improved on SPA itself, as ACM-GPP-ET is an emulation of SPA, therefore the difference should not be viewed as significant. The improved statistics found for ACM-GPP-ET are likely due to a combination of factors underlying errors which by chance lead to an apparent improvement. One exception to this assumption is that SPA's sub-daily meteorological drivers were gap filled based on down-scaled reanalysis drivers (as used in the calibration process) which as noted in the introduction can introduce errors comparable in magnitude to the direct daily aggregation (e.g., Williams et al., 2001a). Finally, as hypothesised SPA and ACM-GPP-ET performed best at forests sites, with some grassland, cropland and woody savanna sites performing less well (Figure 6). The relative pattern of performance between vegetation types is consistent between ACM-GPP-ET and SPA, strongly indicating consistent underlying response to a wide range of climate conditions and ecological states, and similar predictive capabilities when applied in circumstances without site-specific information.

The ACM-GPP-ET predictions used a single, global calibration, and thus evaluated a single response surface to FLUXNET data, without taking into account any ecological variation in plant processes among FLUXNET sites beyond LAI, fine root biomass and soil textural information (potential errors in these components is discussed below). Thus, critical plant traits, such as the maximum rate of carboxylation per leaf area (Vcmax), stem hydraulic conductance (G_p) and rooting depth, were set the same across all sites for SPA and ACM-GPP-ET. But, we expect these parameters to vary, given our knowledge of trait variation at sites and from worldwide studies (Wright et al., 2004; Kattge et al., 2011; Johnson et al., 2018). So, the global parameterisation is likely to be biased for most sites. The poorer performance of SPA and ACM-GPP-ET in predicting GPP in evergreen deciduous forests is likely linked to a bias in parameters, for example (Figure 5). For a more robust global application, ACM-GPP-ET requires prior estimates for local values of the parameters in Table 3. Based on previous works by Bonan et al. (e.g., 2014) we expect the most important local parameterisation will be for root resistivity, plant conductivity and NUE. Root resistivity and plant conductance determine the maximum rates of water transport to the canopy. NUE determines the capacity of carboxylation and electron transport in photosynthesis.

Errors in the LAI, fine root biomass and soil textural information used in the SPA and ACM-GPP-ET model inputs are also likely. Errors in the remote sensing of LAI assimilated within the CARDAMOM framework will propagate into the resulting estimates of LAI and fine root biomass. Soil textural information comes from the HWSD database the errors for which are poorly described. Furthermore, we made assumptions about root depth and canopy height which are also likely biased. LAI information ultimately comes from MODIS (or other satellite products) which has varied skill depending on vegetation cover type (Yan et al., 2016). Yan et al. (2016) showed MODIS LAI detects LAI dynamics least well over forests (particularly needle-leaf), but perhaps more critically for our analysis they also showed a consistent RMSE between 0.6-0.8 m^2/m^2 between vegetation types. For arable crop land and grassland such an RMSE could constitute an error in the magnitude of LAI on the order of 66 % (in their observation dataset), potentially resulting in substantial errors and bias in estimation of ecosystem fluxes.

6.4 Comparison to other global GPP and ET estimates

We aimed for and achieved ACM-GPP-ET's performance against FLUXNET2015 sites ~~is~~to be comparable to that demonstrated by GPP and ET estimates generated by a range of alternate approaches and temporal resolutions (e.g., Jung et al., 2011; Mu et al., 2011; Martens et al., 2017; Wang et al., 2017). For example, FLUXCOM uses a machine learning approach assimilation and a wide range of global spanning information to estimate monthly GPP (Number of sites not reported, $R^2 = \sim 0.82$, RMSE = $\sim$1.18 $gC/m^2/day$) and ET (Number of sites not reported, $R^2 = \sim 0.86$, RMSE = $\sim$0.47 $kgH_2O/m^2/day$) (Jung et al., 2011). At monthly time scales FLUXCOM performs marginally better at estimation of variation in fluxes but with RMSEs roughly half that found with ACM-GPP-ET for both GPP and ET; this is not unexpected as FLUXCOM was calibrated against the FLUXNET database itself (Jung et al., 2011). Whereas the satellite-based remotely sensed derived 8-day MODIS estimates, based on absorbed radiation and empirical response functions, perform less favourably than ACM-GPP-ET for both GPP (18 sites, $R^2 = 0.52$, RMSE = 0.96 $gC/m^2/day$; Wang et al., 2017) and ET (46 sites, $R^2 = 0.65$, RMSE = 0.84 $kgH_2O/m^2/day$; Mu et al., 2011). Finally, GLEAM estimates of ET performed similarly to those achieved by ACM-GPP-ET; GLEAM makes use of a comparatively complex approach to estimate ET, using a model of ecosystem water cycling updated by satellite based remotely sensed information within a data assimilation framework to generate a daily estimate of the global water budget (63 sites, $R^2 = 0.64$, RMSE = 0.73 $kgH_2O/m^2/day$; Martens et al., 2017). In each case the approaches highlighted above made use of vegetation-type-specific information or location-specific remotely sensed biophysical information to drive their analysis compared to our comparatively naive approach using a single set of ecophysiological parameters. Therefore, we reasonably expect that significant improvements through the inclusion of location- and / or vegetation-type-specific calibration as would be achieved through model-data fusion approaches (e.g., Bloom et al., 2016). A key benefit of our process-orientated approach is that unlike the above described approaches, which are each dependent on the input of remotely sensed information, our modelling framework can be used predictively to extrapolate into space and times where remotely sensed information are not available. This is particularly true when ACM-GPP-ET has been coupled to our DALEC C-cycle model allowing for feedbacks between carbon supply and available LAI. Further details on the potential of this coupling below.

6.5 Global Applications

It is typical to generate regional and global estimates of carbon and water cycling using complex land surface models. Such models make vital contributions to assessments of the global carbon budget (Le Quéré et al. , 2015) and weather and climate forecasts. A challenge for these models is that their complexity generates high computational demand, and they have demanding parameterisation needs. Thus, these models are often applied using plant functional type approaches, whereby parameters are set for an entire biome, with no variation and no uncertainty is attached. There is a need then for models of intermediate complexity that are less demanding computationally, have fewer parameters, but retain realism.

ACM-GPP-ET is such a model, constructed from the simplification of a complex land surface model with a long evaluation history, SPA. ACM-GPP-ET captures the critical functional forms in carbon-water interactions the emerge from process representation at sub-canopy, hourly timescales. ACM-GPP-ET can represent the interactions of supply and demand on stomatal opening, and how this responds to changes in atmospheric conditions and soil moisture states. This level of detail is critical for application in global change analyses that are vital for diagnosing and predicting earth system evolution. Thus, ACM-GPP-ET produces realistic outputs, based on comparison with its more complex pre-cursor.

ACM-GPP-ET is well suited for ensemble modelling schemes due to its faster run-time, as shown in the MH-MCMC calibration process used here with SPA outputs used as training data. The parameter posteriors generated here (Figure A1) provide a starting point for full carbon cycle and water cycle analyses across regional to global domains. For instance, Bloom et al. (2016) have shown how an IC GPP model, ACM-GPP (Williams et al., 1997), combined with a carbon cycling model (DALEC; Williams et al., 2005), can be linked into a model-data fusion framework, CARDAMOM. CARDAMOM can, when combined with DALEC, retrieve probabilistic estimates of carbon stocks, fluxes and model parameters (including key unknowns such as photosynthate allocation to plant tissues and their residence times). CARDAMOM can produce outputs across a domain at the resolution of input forcing (climate data, burned area) and observational constraints (satellite time series of LAI, biomass maps, soil C maps). The advantage of CARDAMOM is that it generates likelihoods for model initial conditions and parameter values that are consistent with climate forcing and domain observations from e.g. satellites, and their estimated errors. Currently CARDAMOM infers water limitations to C cycling through satellite observations of greenness alone. Because there is no coupling to a local water model, CARDAMOM cannot use modelled information on water balance, or independent observations such as surface soil moisture (e.g., Chen et al., 2018). Through using ACM-GPP-ET in CARDAMOM, it will be possible to assimilate new observational data related to water fluxes and state variables.

The combination of ACM-GPP-ET, coupled to DALEC, and CARDAMOM provide multiple direct and indirect avenues for propagating information acquired using intermediate complexity models to complex state-of-the-art TEMs. ACM-GPP-ET and SPA directly share 5 parameters calibrated in this study (Table 2) plus a further 9 biophysical traits which where not calibrated in this study (Table 3). Moreover, all of the parameters calibrated in this study (Table 2) can be indirectly related to those used in SPA (and many other TEMs) e.g., NUE which is closely related to Vcmax, Jmax and foliar nitrogen, but also radiation absorption/reflectance as a function of LAI. Similarly, when ACM-GPP-ET is combined with DALEC and used within the CARDAMOM framework analyses such as those carried out by Bloom et al. (2016) (as is intended) retrieving information on carbon stocks, carbon allocation and residence times results in the retrieval of ecologically relevant traits. These traits can be directly related to parameters found in most state-of-the-art TEMs equipped with a C-cycle. Such information should at a minimum provide information on spatial variation expected and in the optimum situation inform on the exact magnitude of those parameters.

6.6 Further opportunities and gaps

There are an array of next steps to undertake for further development both as a stand alone tool and as part of a coupled modelling framework along with DALEC and CARDAMOM. The ACM-GPP-ET parameters estimated here against SPA can be calibrated individually at FLUXNET2015 site (were sufficient biophysical information are available) to determine critical parameter variability to explain observed differences in fluxes. Driven with remotely sensed LAI ACM-GPP-ET could ~~It would be possible to~~make global ~~interpolated~~estimates of GPP, ET and WUE for direct comparison with outputs from FLUXCOM, GLEAM and CMIP5 model ensembles. As part of the CARDAMOM framework a site specific FLUXNET2015 analysis allows us to assess our ability to retrieve information on the whole carbon cycle across ecological and climate gradients within a data-rich environment, including key unknowns such as rooting depths which play a critical role in ecosystem resilience to drought. Such analyses provide the supporting frameworks needed to conduct global scale reanalyses and potentially near-term (next 12 months) and intermediate term (next 10 years) predictions with fully resolved uncertainties due to the propagation of ensembles.

Due to lack of space we have not reviewed the uncertainty estimates on parameter retrievals in the calibration of ACM-GPP-ET from SPA, but these contain useful information on the relative uncertainties in key processes in the aggregation. There are gaps in the capacity of ACM-GPP-ET globally; C4 pathways have not been included, nor organic soils. However, SPA is capable of simulating flux responses to these process adjustments, so new calibrations and/or model structure can be generated following a similar approach to that laid out here.

7 Conclusions

We have calibrated and robustly validated a model of intermediate complexity ACM-GPP-ET demonstrating good capacity of simulating the carbon-water dynamics of a state-of-the-art SPA model. ACM-GPP-ET has demonstrated substantial predictive skill when simulating fully independent eddy covariance derived estimates of carbon and water exchange which is comparable to that of other globally used GPP and ET products. Finally, ACM-GPP-ET is highly computationally efficient, $\sim$2200 times faster than SPA, opening up a substantial range of further opportunities.

Code availability. The code for ACM-GPP-ET version 1 has been made freely available from the Edinburgh DataShare (doi: http://hdl.handle.net/10283/3237). Subsequent source code developments will be made available under GNU General Public License (GPL) via Github (link will be made available in the final published manuscript). The Fortran source code for the Weather Generator v1 used when downscaling daily meteorology to hourly time step is available here https://github.com/GCEL/WeatherGenerator_v1.

Appendix A: Appendix A: Calibrated parameter distributions

The CARDAMOM calibration process of ACM-GPP-ET retrieves multiple parameter sets consistent with the calibration dataset, resulting in a probability density function (PDFs) for each parameter. A detailed discussion of the PDFs retrieved is out of scope for this study, however a brief description of the primary features is given below (Figure A1).

The width (relative to the prior range) and overall shape of the PDF (i.e. uni- or multi-modal) gives an indication of the constraint achieved. The majority of parameter posteriors (16 out of 22) cover less than 50 % of their prior range and show a single clear peak value without substantial skew (e.g. NUE; Figure A1). Notable exception include aPAR_trans and kPAR_refl, indicating that there is a degree of equifinality in absorption the required PAR to support photosynthesis and canopy evaporation. Therefore, providing a potential focus for refinement of the model or calibration process (e.g. through the introduction of new data streams).

Appendix B: Appendix B: SPA ecophysiological parameters

Author contributions. TLS coded the model and conducted the analysis. Both TLS and MW developed the experimental design and wrote the manuscript

Competing interests. The authors declare that they have no competing interests.

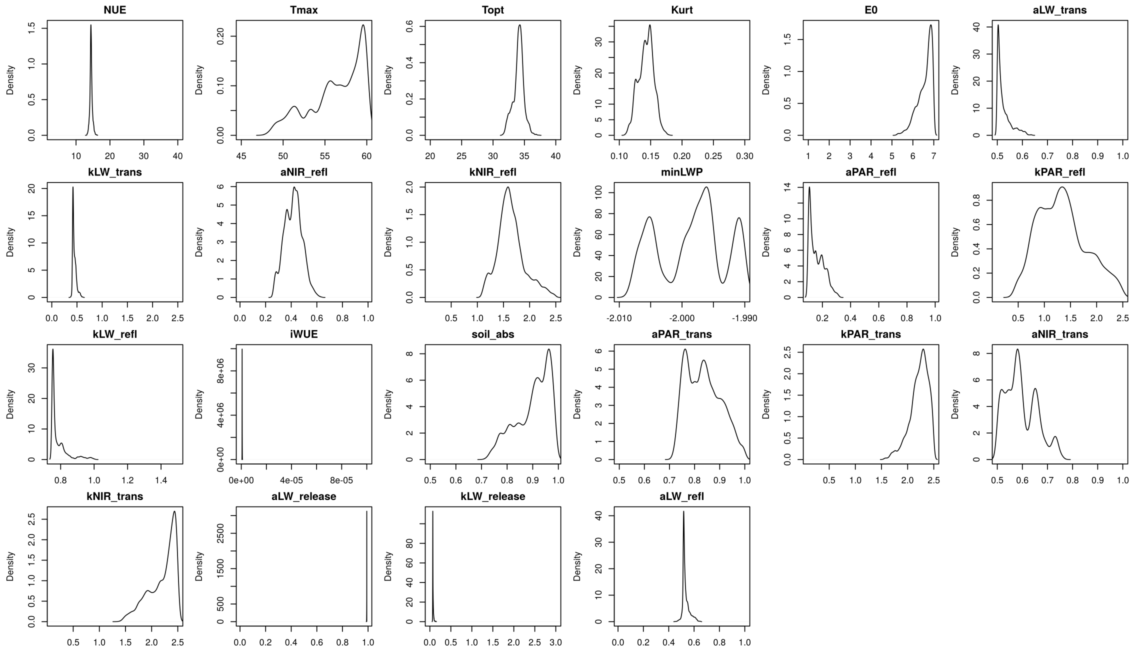

Figure A1. Probability density functions of the retrieved parameters for ACM-GPP-ET. The figure label refers to the name given in Table 1 of the main text. The range of the x-axis matches that of the parameter prior ranges to allow easy identification of those parameters which are the easiest to constrain.

Table B1. Ecophysiological parameters used by SPA within this study but not already provided in Table 2 and 3. These parameters are drawn from previous SPA publications (Williams et al., 1996; Bonan et al., 2014).

Symbol	Value	Units	Description
κC	33.6	μmolC/gN/s	Coefficient relating the maximum rate of carboxylation to leaf nitrogen content
κJ	53.8	μmolC/gN/s	Coefficient relating the maximum rate of electron transport to leaf nitrogen content
minLWP$_{spa}$	2	MPa	Absolute value for minimum tolerated leaf water potential
Leaf$_{c}ap$	2500	mmolH$_2$O/m$^2_{leafarea}$/MPa	Leaf / plant water capacitance for supply versus demand calculation
leaf$_{p}arrefl$	0.16	fraction	Leaf level reflectance of incident photosynthetically active radiation
leaf$_{p}artrans$	0.16	fraction	Leaf level transmittance of photosynthetically active radiation
leaf$_{n}irrefl$	0.43	fraction	Leaf level reflectance of incident near-infrared radiation
leaf$_{n}irtrans$	0.26	fraction	Leaf level transmittance of near-infrared radiation
soil$_{p}arrefl$	0.03	fraction	Reflectance of photosynthetically active radiation incident on soil surface
soil$_{n}irrefl$	0.02	fraction	Reflectance of near-infrared radiation incident on soil surface

Acknowledgements. This work used eddy covariance data (FLUXNET2015) acquired and shared by the FLUXNET community, including these networks: AmeriFlux, AfriFlux, AsiaFlux, CarboAfrica, CarboEuropeIP, CarboItaly, CarboMont, ChinaFlux, Fluxnet-Canada, GreenGrass, ICOS, KoFlux, LBA, NECC, OzFlux-TERN, TCOS-Siberia, and USCCC. The ERA-Interim reanalysis data are provided by

ECMWF and processed by LSCE. The FLUXNET eddy covariance data processing and harmonization was carried out by the European Fluxes Database Cluster, AmeriFlux Management Project, and Fluxdata project of FLUXNET, with the support of CDIAC and ICOS Ecosystem Thematic Center, and the OzFlux, ChinaFlux and AsiaFlux offices. The study has been supported by the TRY initiative on plant traits (http://www.try-db.org). The TRY initiative and database is hosted, developed and maintained by J. Kattge and G. Bönisch (Max Planck Institute for Biogeochemistry, Jena, Germany). TRY is currently supported by DIVERSITAS/Future Earth and the German Centre for Integrative Biodiversity Research (iDiv) Halle-Jena-Leipzig. This work was funded primarily through the NERC GHG program GREENHOUSE project (grant NE/K002619/1) and the UK Space Agency Forests2020 project (https://ecometrica.com/space/forests2020). Additional resources were provided by the NERC National Centre for Earth Observations (NCEO).

References

Beers, C., Ciais, P., Reichstein, M., Baldocchi, D., Law, B. E., Papale, D, Soussana, J. F., Ammann, C., Buchmann, N., Frank, D., Gianelle, D., Janssens, I. A, Knohl, A., Koestner, B., Moors, E., Roupsard, O., Verbeeck, H., Vesala, T., Williams, C. A., and Wohlfahrt, G.: Temporal and among-site variability of inherent water use efficiency at the ecosystem level, *Global Biogeochem. Cy.*, **23**, https://doi.org/10.1029/2008GB003233, 2009.

Bloom, A. A., and M. Williams (2015), Constraining ecosystem carbon dynamics in a data-limited world: integrating ecological "common sense" in a model-data-fusion framework., *Biogeosciences*, *12*, 1299–1315, https://doi.org/10.5194/bg-12-1299-2015.

Bloom, A. A., J.-F. Exbrayat, I. R. van der Velde, L. Feng, and M. Williams (2016), The decadal state of the terrestrial carbon cycle: Global retrievals of terrestrial carbon allocation, pools, and residence times, *P. Natl. Acad. Sci. USA*, *113*(5), 1285–1290, https://doi.org/10.1073/pnas.1515160113.

Blyth, E. M., and C. C. Daamen (1997), The accuracy of simple soil water models in climate forecasting., *Hydrology and Earth System Sciences*, *1*(2), 241–248, https://doi.org/10.5194/hess-1-241-1997.

Bonan, G. B., M. Williams, R. A. Fisher, and K. W. Oleson (2014), Modeling stomatal conductance in the earth system: linking leaf water-use efficiency and water transport along the soil-plant-atmosphere continuum, *Geosci. Model Dev.*, *7*(5), 2193–2222, https://doi.org/10.5194/gmd-7-2193-2014.

Bonan, G. B. and Doney, S, C.: Climate, ecosystems, and planetary futures: The challenge to predict life in Earth system models, *Science*, **359**, 6375, doi:10.1126/science.aam8328, 2008.

Bonan, G. B., Patton, E. G., Harman, I. N., Oleson, K. W., Jinnigan, J. J., Lu, Y. and E.A. Burakoski (2013), Modeling canopy-induced turbulence in the Earth system: a unified parameterization of turbulent exchange within plant canopies and the roughness sublayer (CLM-ml v0), *Geosci. Model Dev.*, **11**, 1467–1496, https://doi.org/10.5194/gmd-11-1467-2018.

Buckley, T. N., Cescatti, A., and G.D. Farquhar (2013), What does optimization theory actually predict about crown profiles of photosynthetic capacity when models incorporate greater realism?, *Plant Cell Environ.*, **36**, 1547–1563, https://doi.org/10.1111/pce.12091.

Chen, F., Crow, W. T., Bindlish, R., Colliander, A., Burgin, M. S., Asanuma, J., and K. Aida (2018), Global-scale evaluation of SMAP, SMOIS, ASCAT soil moisture products, *Remote Sens. Environ.*, **214**, 1–13, https://doi.org/10.1016/j.rse.2018.05.008.

Coble, A. P., VanderWall, B., Mau, A., and M.A. Cavaleri (2016), How vertical patterns in leaf traits shift seasonally and the implications for modelling canopy photosynthesis in a temperate deciduous forest., *Tree Physiol.*, **36**, 1077–1091, https://doi.org/10.1093/treephys/twp043.

Collatz, G., Ball, J., Grivet, C., and Berry, J.: Physiological and environmental-regulation of stomatal conductance, photosynthesis and transpiration – a model that includes laminar boundary-layer, *Agr. Forest Meteorol.*, **54**, 107–136, doi:10.1016/0168-1923(91)90002-8, 1991.

Dee, D. P., Uppala, S. M., Simmons, A. J., Berrisford, P., Poli, P., Kobayashi, S., Andrae, U., Balmaseda, M. A., Balsamo, G., Bauer, P., Bechtold, P., Beljaars, A. C. M., van de Berg, L., Bidlot, J., Bormann, N., Delsol, C., Dragani, R., Fuentes, M., Geer, A. J., Haimberger, L., Healy, S. B., Hersbach, H., Hólm, E. V., Isaksen, L., Kållberg, P., Köhler, M., Matricardi, M., McNally, A. P., Monge-Sanz, B. M., Morcrette, J.-J., Park, B.-K., Peubey, C., de Rosnay, P., Tavolato, C., Thépaut, J.-N. and Vitart, F. (2011), The ERA-Interim reanalysis: configuration and performance of the data assimilation system,*Q. J. Roy. Meteor. Soc.*, **137**, 553–597, https://doi.org/10.1002/qj.828.

Fan, Y., Miguez-Macho, G., Jobbágy, E. G., Jackson, R. B., and C. Otero-Casal (2017), Hydrologic regulation of plant rooting depth., *P. Natl. Acad. Sci. USA*, https://doi.org/10.1073/pnas.1712381114.

Farquhar, G. D. and von Caemmerer, S.: Modelling of photosynthetic response to the environment, in: Physiological Plant Ecology II, Encyclopedia of Plant Physiology, Springer-Verlag, Berlin, 1982.

Fisher, R.A., Williams, M., Do Vale, R.L., Da Costa, A.L. and Meir, P.: Evidence from Amazonian forests is consistent with isohydric control of leaf water potential, *Plant Cell Environ.*, **29**, 151–165, https://doi.org/10.1111/j.1365-3040.2005.01407.x, 2006.

Fisher, R.A., Williams, M., Da Costa, A.L., Malhi, Y., Da Costa, R.F., Almeida, S. and Meir, P.: The response of an Eastern Amazonian rain forest to drought stress: results and modelling analyses from a throughfall exclusion experiment, *Glob. Change Biol.*, **13**, 2361–2378, https://doi.org/10.1111/j.1365-2486.2007.01417.x, 2007.

Fisher, R. A., M. Williams, M. de Lourdes, A. L. de Costa, and P. Meir (2008), Evaluating climatic and soil water controls on evapotranspiration at two Amazonian rainforest sites, *Agr. Forest Meteorol.*, *148*, 850–861.

Fer, I, Kelly, R., Moorcroft, P.R., Richardson, A.D., Cowdery, E.M., and Dietze, M.C.: Linking big models to big data: efficient ecosystem model calibration through Bayesian model emulation, *Biogeosciences*, **15**, 5801–5830, https://doi.org/10.5194/bg-15-5801-2018, 2018.

Fox, A., Williams, M., Richardson, A.D., Cameron, D., Gove, J.H., Quaife, T., Ricciuto, D., Reichstein, M., Tomelleri, E., Trudinger, C.M., and M.T. Van Wijk (2009), The REFLEX project: Comparing different algorithms and implementations for the inversion of a terrestrial ecosystem model against eddy covariance data, *Agr. Forest Meteorol.*, *149*, 1597-1615, https://doi.org/10.5194/gmd-9-2415-2016.

Garratt, J. R.: The Atmospheric Boundary Layer, Cambridge University Press, Cambridge, UK, 1992.

Ghimire, B., Riley, W.J., Koven, C.D., Kattge, J., Rodgers, A., Reich, P., and Wright, I.J.: A global trait-based approach to estimate leaf nitrogen functional allocation from observations, *Ecol. Appl.*, **27**, 1421–1434, 2017.

Harman, I. N. and Finnigan, J. J.: A simple unified theory for flow in the canopy and roughness sublayer, *Bound. Lay. Meteorol.*, **123**, 339–363, 2007.

Harper, A. B., Cox, P. M., Friedlingstein, P., Wiltshire, A. J., Jones, C. D., Sitch, S., Mercado, L. M., Groenendijk, M., Robertson, E., Kattge, J., Boenisch, G., Atkin, O. K., Bahn, M., Cornelissen, J., Niinemets, U., Onipchenko, V., Penuelas, J., Poorter, L., Reich, P. B., Soudzilovskaia, N. A. and van Bodegom, P.: Improved representation of plant functional types and physiology in the Joint UK Land Environment Simulator (JULES v4.2) using plant trait information, *Geosci. Model Dev.*, **9**, (7), 2415–2440, https://doi.org/10.5194/gmd-9-2415-2016, 2016.

Hiederer, R., and M. Köchy (2011), Global soil organic carbon estimates and the harmonized world soil database, *EUR*, *79*(25225), https://doi.org/10.2788/13267.

Johnson, D.M., Berry, Z.C., Baker, K.V., Smith, D.D., McCulloch, K.A., and Domec, J.C.: Leaf hydraulic parameters are more plastic in species that experience a wider range of leaf water potentials, *Funct Ecol.*, **32**, 894–903, 2018.

Jones, H. G.: Plants and Microclimate, Cambridge University Press, Cambridge, 1992.

Jung, M., Reichstein, M., Margolis, H.A., Cescatti, A., Richardson, A.D., Arain, M.A., Arneth, A., Bernhofer, C., Bonal, D., Chen, J., Gianelle, D., Gobron, N., Kiely, G., Kutsch, W., Lasslop, G., Law, B.E., Lindroth, A., Merbold, L., Montagnani, L., Moors, E.J., Papale, D., Sottocornola, M., Vaccari, F. and Williams, C.: Global patterns of land-atmosphere fluxes of carbon dioxide, latent heat, and sensible heat derived from eddy covariance, satellite, and meteorological observations, *J. Geophys. Res-Biogeo.*, **116**, G00J07, https://doi.org/10.1029/2010JG001566, 2011.

Kaimal, J. C. and Finnigan, J. J.: Atmospheric Boundary Layer Flows: Their Structure and Measurement, Oxford University Press, 200 Madison Avenue, NY 10016, USA and Oxford University, Oxford UK, 1994.

Kattge, J., Dìaz, S., Lavorel, S., Prentice, I. C., Leadley, P., Bönisch, G., Garnier, E., Westoby, M., Reich, P. B., Wright, I. J., Cornelissen, J. H. C., Violle, C., Harrison, S. P., Van Bodegom, P. M., Reichstein, M., Enquist, B. J., Soudzilovskaia, N. A., Ackerly, D. D., Anand, M., Atkin, O., Bahn M., Baker, T. R., Baldocchi, D., Bekker, R., Blanco, C. C., Blonder, B., Bond W. J., Bradstock, R., Bunker, D. E., Casanoves, F., Cavender-Bares, J., Chambers, J. Q., Chapin III, F. S., Chave, J., Coomes, D., Cornwell, W. K., Craine, J. M., Dobrin, B. H., Duarte, L., Durka, W., Elser, J., Esser, G., Estiarte, M., Fagan W. F., Fang, J., Fernàndez-Mèndez, F., Fidelis, A., Finegan, B., Flores, O., Ford, H., Frank, D., Freschet, G. T., Fyllas, N. M., Gallagher, R. V., Green, W. A., Gutierrez, A. G., Hickler, T., Higgins, S. I., Hodgson, J. G., Jalili, A., Jansen, S., Joly, C. A., Kerkhoff, A. J., Kirkup, D., Kitajima, K., Kleyer, M., Klotz, S., Knops, J. M. H., Kramer, K., Kühn, I., Kurokawa, H., Laughlin, D., Lee, T. D., Leishman, M., Lens, F., Lenz, T., Lewis, S. L., Lloyd, J., Llisià, J., Louault, F., MA, S., Mahecha, M. D., Manning, P., Massad, T., Medlyn, B. E., Messier, J., Moles, A. T., Müller, S. C., Nadrowski, K., Naeem, S., Niinemets, Ü., Nöllert, S., Nüske, A., Ogaya, R., Oleksyn, J., Onipchenko, V. G., Onoda, Y., Ordoñez, J., Overbeck, G., Ozinga, W. A., Patiño, S., Paula, S., Pausas, J. G., Peñuelas, J., Phillips, O. L., Pillar, V., Poorter, H., Poorter, L., Poschlod, P., Prinzing, A., Proulx, R., Rammig, A., Reinsch, S., Reu, B., Sack, L., Salgado-Negret, B., Sardans, J., Shiodera, S., Shipley, B., Siefert, A., Sosinski, E., Soussana, J.-F., Swaine, E., Swenson, N., Thompson, K., Thornton, P., Waldram, M., Weiher, E., White, M., White, S., Wright, S. J., Yguel, B., Zaehle, S., Zanne, A. E. and Wirth, C.: TRY ? a global database of plant traits, *Glob. Change Biol.*, **17**, 9, 2905–2935, https://doi.org/10.1111/j.1365-2486.2011.02451.x, 2011.

Keenan, T.F., Hollinger, D.Y., Bohrer, G., Dragoni, D., Munger, J.W., Schmid, H.P. and Richardson, A.D.: Increase in forest water-use efficiency as atmospheric carbon dioxide concentrations rise, *Nature*, **499**, 7458, https://doi.org/10.1038/nature12291, 2013.

Knauer, J., Zaehle, S., Reichstein, M., Medlyn, B. E., Forkel, M., Hagemann, S., and Werner, C.: The response of ecosystem water-use efficiency to rising atmospheric CO2 concentrations: sensitivity and large-scale biogeochemical implications, *New Phytol.*, **213**,(4), 1654-1666, https://doi.org/10.1111/nph.14288, 2017.

Krinner, G and Viovy, N and de Noblet-Ducoudre, N and Ogee, J and Polcher, J and Friedlingstein, P and Ciais, P and Sitch, S and Prentice, IC: A dynamic global vegetation model for studies of the coupled atmosphere-biosphere system, *Global Biogeochem. Cy.*, **19**, GB1015, https://doi.org/10.1029/2003GB002199, 2005.

Kuppel, S, Peylin, P., Chevallier, F., Bacour, C., Maignan, F., and Richardson, A.D.: Constraining a global ecosystem model with multi-site eddy-covariance data, *Biogeosciences*, **9**, 3757–3776, https://doi.org/10.5194/bg-9-3757-2012, 2012.

López-Blanco, E., Lund, M., Christensen, T.R., Tamstorf, M.P., Smallman, T.L., Slevin, D., Westergaard-Nielsen, A., Hansen, B.U., Abermann, J. and Williams, M., Plant Traits are Key Determinants in Buffering the Meteorological Sensitivity of Net Carbon Exchanges of Arctic Tundra, *J. Geophys. Res-Biogeo.*, https://doi.org/10.1029/2018JG004386, 2018.

Le Quéré, C., R. Moriarty, R. M. Andrew, J. G. Canadell, S. Sitch, J. I. Korsbakken, P. Friedlingstein, G. P. Peters, R. J. Andres, T. A. Boden, R. A. Houghton, J. I. House, R. F. Keeling, P. Tans, A. Arneth, D. C. E. Bakker, L. Barbero, L. Bopp, J. Chang, F. Chevallier, L. P. Chini, P. Ciais, M. Fader, R. A. Feely, T. Gkritzalis, I. Harris, J. Hauck, T. Ilyina, A. K. Jain, E. Kato, V. Kitidis, K. Klein Goldewijk, C. Koven, P. Landschützer, S. K. Lauvset, N. Lefèvre, A. Lenton, I. D. Lima, N. Metzl, F. Millero, D. R. Munro, A. Murata, J. E. M. S. Nabel, S. Nakaoka, Y. Nojiri, K. O'Brien, A. Olsen, T. Ono, F. F. Pérez, B. Pfeil, D. Pierrot, B. Poulter, G. Rehder, C. Rödenbeck, S. Saito, U. Schuster, J. Schwinger, R. Séférian, T. Steinhoff, B. D. Stocker, A. J. Sutton, T. Takahashi, B. Tilbrook, I. T. van der Laan-Luijkx, G. R. van der Werf, S. van Heuven, D. Vandemark, N. Viovy, A. Wiltshire, S. Zaehle, and N. Zeng (2015), Global carbon budget 2015, *Earth System Science Data*, *7*(2), 349–396, https://doi.org/10.5194/essd-7-349-2015.

Martens, B., Miralles, D. G., Lievens, H., van der Schalie, R. and deJeu, R.A.M.: GLEAM v3: satellite-based land evaporation and root-zone soil moisture, *Geosci. Model Dev.*, **10**, 1903–1925, https://doi.org/10.5194/gmd-10-1903-2017, 2017.

Mauder, M., Cuntz, M., Drüe, C., Graf, A., Rebmann, C., Schmid, H. P., Schmidt, M. and Steinbrecher, R.: A strategy for quality and uncertainty assessment of long-term eddy-covariance measurement, *Agr. Forest Meteorol.*, **169**, 122–135, 2013.

McMurtie, R. R., Comins, H. N., Kirschbaum, M. U. F. and Wang, Y. P.: Modifying existing forest growth models to take account of effects of elevated CO_2, *Aust. J. Bot.*, **40**, 657–677, 1992.

Medlyn, B.E, Duursma, R. A., Eamus, D., Ellsworth, D.S., Prentice, I.C., Barton, C.V.M., Crous, K.Y., De Angelis, P., Freeman, M. and Wingate, L.: Reconciling the optimal and empirical approaches to modelling stomatal conductance, *Glob. Change Biol.*, **17**, 6, 2134–2144, https://doi.org/10.1111/j.1365-2486.2010.02375.x, 2011.

Monteith, J. L.: Evaporation and environment. In Symposia of the Society for Experimental Biology, **19**, pp. 205-234, Cambridge University Press, Cambridge, 1965.

Mu, Q., Zhao, M. and Running, S.W.: Improvements to a MODIS global terrestrial evapotranspiration algorithm, *Remote. Sens. Environ.*, **115**, 1781–1800, https://doi.org/10.1016/j.rse.2011.02.019, 2011.

Nikolov, N., Massman, W., and Schoettle, A.: Coupling biochemical and biophysical processes at the leaf level – an equilibrium photosynthesis model for leaves of C-3 plants, *Ecol. Model.*, **80**, 205–235, 1995.

Niu, G. Y. and Yang, Z. L.: Effects of vegetation canopy processes on snow surface energy and mass,*J. Geophys. Res.*, **109**, D23111, doi:10.1029/2004JD004884, 2004.

Nolan, R.H., Tarin, T., Santini, N.S., McAdam, S.A.M., Ruman, R., and Eamus, D.: Differences in osmotic adjustment, foliar abscisic acid dynamics, and stomatal regulation between an isohydric and anisohydric woody angiosperm during drought, Plant, Cell & Environment, 40, 1365–3040, 2017, https://doi.org/10.1111/pce.13077.

Oleson, K. W., Lawrence, D. M., Bonan, G. B., Flanner, M. G., Kluzek, E. K., Lawrence, P. J., Levis, S., Swenson, S. C., and Thornton, P. E.: Technical Description of version 4.0 of the Community Land Model (CLM), NCAR/TN-478+STR, Climate and Global Dynamics Division, National Center for Atmospheric Research, Boulder, Colorado, 2010.

Priestley, C. H. B. and Taylor, R. J.: On the assessment of surface heat flux and evaporation using large-scale parameters, *Mon. Weather Rev.*, **100**, 81–92, 1992.

Poyatos, R., Granda, V., Molowny-Horas, R., Mencuccini, M., Steppe, K. and J. Martinez-Vilalta (2016), SAPFLUXNET: towards a global database of sap flow measurements, *Tree Physiology*, **36**, 1449–1455, https://doi.org/10.1093/treephys/tpw110.

Raoult, N.N., Jupp, T.E., Cos, P.M., and C.M. Luke (2016), Land-surface parameter optimisation using data assimilation techniques: the adJULES system V1.0., *Geoscientific Model Development*, **9**, 2833–2852, https://doi.org/10.5194/gmd-9-2833-2016.

Raupach, M. R.: Simplified expressions for vegetation roughness length and zero-plane displacement as functions of canopy height and area index, *Bound. Lay. Meteorol.*, **71**, 211–216, 1994.

Saxton, K. E., Rawls, W. J., Romberger, J. S., and Papendick, R. I.: Estimating generalized soil-water characteristics from texture, *Soil Sci. Soc. Am. J.*, **90**, 1031–1036, 1986.

Scartazza, A., Di Baccio, D., Bertolotto, P., Gavrichkova, O. and G. Matteucci (2016), Investigating the European beech (*Fagus sylvatica* L.) leaf characteristics along the vertical canopy profile: leaf structure, photosynthetic capacity, light energy dissipation and photoprotection mechanisms., *Tree Physiol.*, **36**, 1060–1076, https://doi.org/10.1093/treephys/tpw038.

Smallman, T. L., Moncrieff, J. B., and Williams, M.: WRFv3.2-SPAv2: development and validation of a coupled ecosystem-atmosphere model, scaling from surface fluxes of CO_2 and energy to atmospheric profiles, *Geosci. Model Dev.*, **6**, 1079–1093, https://doi.org/10.5194/gmd-6-1079-2013, 2013.

Smallman, T. L., Williams, M., and Moncrieff, J. B.: Can seasonal and interannual variation in landscape CO_2 fluxes be detected by atmospheric observations of CO_2 concentrations made at a tall tower?, *Biogeosciences*, **11**, 735–747, https://doi.org/10.5194/bg-11-745-2014, 2014.

Smallman, T.L., J.-F. Exbrayat, M. Mencuccini, A.A. Bloom, A.A., and M. Williams (2017), Assimilation of repeated woody biomass observations constrains decadal ecosystem carbon cycle uncertainty in aggrading forests, *J. Geophys. Res-Biogeo.*, **122**, https://doi.org/10.1002/2016JG003520.

Stoy, P. C., Katul, G. G., Siqueira, M. B. S., Juang, J.-Y., Novick, K. A., Uebelherr, J. M., and R. Oren (2006), An evaluation of models for partitioning eddy covariance-measured net ecosystem exchange into photosynthesis and respiration, *Agr. Forest Meteorol.*, *141*(1), 2–18, https://doi.org/10.1016/j.agrformet.2006.09.001.

Sun, Y., Gu, L., Dickinson, R. E., Norby, R. J., Pallardy, S. G., and F.M. Hoffman (2014), Impact of mesophyll diffusion on estimated global land CO2 fertilization., *Proceedings of the National Academy of Sciences*, https://doi.org/10.1073/pnas.1418075111.

Sus, O., Williams, M., Bernhofer, C., Beziat, P., Buchmann, N., Ceschia, E., Doherty, R., Eugster, W., Gruenwald, T., Kutsch, W., Smith, P., and Wattenbach, M.: A linked carbon cycle and crop developmental model: description and evaluation against measurements of carbon fluxes and carbon stocks at several European agricultural sites, *Agr. Ecosyst. Environ.*, **139**, 402–418, 2010.

Swann, A. L. S., Hoffman, F. M., Koven, C. D., and Randerson, J. T.: Plant responses to increasing CO2 reduce estimates of climate impacts on drought severity, Proceedings of the National Academy of Sciences, 113, 10019–10024, doi:10.1073/pnas.1604581113, 2016.

Thomas, R.Q., and Williams, M.: A model using marginal efficiency of investment to analyse carbon and nitrogen interactions in terrestrial ecosystems (ACONITE Version 1), *Geoscientific Model Development*, **7**, 2015–2037, https://doi.org/10.5194/gmd-7-2015-2014, 2014.

Tuzet, A., Perrier, A., and Leuning, R.: A coupled model of stomatal conductance, photosynthesis and transpiration, *Plant Cell Environ.*, **26**, 1097–1116, doi:10.1046/j.1365-3040.2003.01035.x, 2003.

Wang, Y. P. and Leuning, R.: A two-leaf model for canopy conductance, photosynthesis and partitioning of available energy I: model description and comparison with a multi-layered model, *Agr. Forest Meteorol.*, **91**, 89–111, 1998.

Wang, L., Zhu, H., Lin, A., Zou, L., Qin, W and Du, Q.: Evaluation of the Latest MODIS GPP Products across Multiple Biomes Using Global Eddy Covariance Flux Data, *Remote Sensing*, **9**, 5, https://doi.org/10.3390/rs9050418, 2017.

Way, D. A., Oren, R., and Y. Kroner (2015), The space-time continuum: the effects of elevated CO2 and temperature on trees and the importance of scaling., *Plant Cell Environ.*, **38**, 991–1007, https://doi.org/10.1111/pce.12527.

Wei, Z., Yoshimura, K., wang, L., Miralles, D. G., Jasechko, S., and X. Lee (2017), Revisiting the contribution of transpiration to global terrestrial evapotranspiration., *Geophys. Res. Lett.*, **44**, 2792–2801, https://doi.org/10.1002/2016GL072235.

Williams, M., Rastetter, E. B., Fernandes, D. N., Goulden, M. L., Wofsy, S. C., Shaver, G. R., Melillo, J. M., Munger, J. W., Fan, S. M., and Nadelhoffer, K. J.: Modelling the soil-plant-atmosphere continuum in a Quercus-Acer stand at Harvard Forest: the regulation of stomatal conductance by light, nitrogen and soil/plant hydraulic properties, *Plant Cell Environ.*, **19**, 911–927, 1996.

Williams, M., E. Rastetter, D. Fernandes, M. Goulden, G. Shaver, and L. Johnson (1997), Predicting gross primary productivity in terrestrial ecosystems, *Ecol. Appl.*, **7**(3), 882–894.

Williams, M., Malhi, Y., Nobre, A., Rastetter, E., Grace, J., and Pereira, M.: Seasonal variation in net carbon exchange and evapotranspiration in a Brazilian rain forest: a modelling analysis, *Plant Cell Environ.*, **21**, 953–968, doi:10.1046/j.1365-3040.1998.00339.x, 1998.

Williams, M., Eugster, W., Rastetter, E., McFadden, J., and Chapin, F.: The controls on net ecosystem productivity along an Arctic transect: a model comparison with flux measurements, *Glob. Change Biol.*, **6**, 116–126, 2000.

Williams, M., Rastetter, E.B., Shaver, G.R., Hobbie, J.E., Carpino, E. and Kwiatkowski, B.L.: Primary production of an arctic watershed: An uncertainty analysis, *Ecological Applications*, **11**, 1800–1816, 2001.

Williams, M., Law, B., Anthoni, P., and Unsworth, M.: Use of a simulation model and ecosystem flux data to examine carbon-water interactions in ponderosa pine, *Tree Physiol.*, **21**, 287–298, 2001.

Williams, M., Schwarz, P. A., Law, B. E., Irvine, J., and Kurpius, M.: An improved analysis of forest carbon dynamics using data assimilation, *Glob. Change Biol.*, **11**, 89–105, 2005.

Wright, I.J., Reich, P.B., Westoby, M., Ackerly, D.D., Baruch Z., Bongers, F., Cavender-Bares, J., Chapin T., Cornelissen, J.H.C., Diemer, M., Flexas, J., Garnier, E, Groom, P.K., Gulias, J, Hikosaka, K., Lamont, B.B., Lee, T., Lee, W., Lusk, C., Midgley, J.J. Navas, M-L, Niinemets, U., Oleksyn, J., Osada, N., Poorter, H., Poot, P., Prior, L., Pyankov, V.I., Roumet, C, Thomas, S.C., Tjoelker, M.G., Veneklaas, E.J. & Villar, R.: The worldwide leaf economics spectrum, *Nature*, **424**, 821-827, https://doi.org/10.1038/nature02403, 2004.

Qin, Z., Berliner, P., and Karnieli, A.: Numerical solution of a complete surface energy balance model for simulation of heat fluxes and surface temperature under bare soil environment, *Appl. Math. Comput.*, **130**, 171–200, 2002.

Yan, K., Park, T., Yan, G., Liu, Z., Yang, B., Chen, C., Nemani, R. R., Knyazikhin, Y., and R.B. Myneni (2016), Evaluation of MODIS LAI/FPAR Product Collection 6. Part 2: Validation and Intercomparison, *Remote Sensing*, **8**, https://doi.org/10.3390/rs8060460.

Ziehn, T., Scholze, M., and W. Knorr (2012), On the capability of Monte Carlo and adjoint inversion techniques to derive posterior parameter uncertainties in terrestrial ecosystem models, *Global Biogeochemical Cycles*, **26**, https://doi.org/10.1029/2011GB004185.